

Evolution of Cooperation under Environmental Variability

Graduate School of Science and Technology
Degree Programs in Systems and Information Engineering
University of Tsukuba

March 2026

Masaaki Inaba

Contents

1	Introduction	1
1.1	Theoretical background	1
1.2	Environmental variability and the evolution of modern human behavior	3
1.3	Environmental variability and the evolution of cooperation	4
1.4	Research objectives and approach	5
1.5	Organization	5
2	The base model	8
2.1	Model	8
2.2	Results	13
2.3	Summary	18
3	The 2-level model with migration	19
3.1	Model	19
3.2	Results	24
3.3	Summary	34
4	The 2-dimensional model with migration	36
4.1	Model	37
4.2	Results	40
4.3	Summary	47
5	Conclusion	49
5.1	Summary and cross-model comparison	49
5.2	Implications and significance	53
5.3	Limitations and future directions	54
5.4	Concluding remarks	57
Appendix		59
Bibliography		61
Acknowledgments		69

List of Figures

2.1	Relationships, geographical structure, and EV	11
2.2	The effect of RV	14
2.3	The effect of UV	15
2.4	The effect of CV	16
2.5	Effects of EV on Cooperation	17
3.1	Illustration of the model structure	21
3.2	Average cooperation rates as functions of p_{EV} and p_M	26
3.3	Standard deviations corresponding to Figure 3.2	27
3.4	Ablation experiments corresponding to Figure 3.2	28
3.5	Temporal evolution of group-level cooperation	29
3.6	Evolution of individual-level cooperation and resource dynamics	30
3.7	Effects of population size parameters	31
3.8	Effects of initial cooperation rate	33
3.9	Effects of initial network weight w_0 and relation weight update rate Δw on cooperation rates	34
4.1	Spatially heterogeneous prosperity patterns generated by SoR(s)	38
4.2	Influence of environmental variability (p_{EV}) and agent mobility (p_M) on the cooperation rate (ϕ_C)	41
4.3	Temporal dynamics under cyclic environmental variability	42
4.4	Temporal dynamics under cyclic environmental variability with low agent mobility	44
4.5	Influence of population size (N) on cooperation rate (ϕ_C)	45
4.6	Temporal dynamics under cyclic environmental variability in the 1-SoR configuration	46
4.7	Central resource-rich areas under $\phi_C^0 = 0.5$ or 1.0	47
4.8	Influence of SoR orientation (p_{SoR}) on the cooperation rate (ϕ_C)	47

List of Tables

1.1	Key concepts used throughout this dissertation	7
2.1	Model parameters used in the simulations	13
3.1	Model parameters used in the simulations	25
4.1	Model parameters used in the simulations	41
5.1	Cross-model comparison of the key features and findings	50
A.1	Detailed comparison of the three simulation models	60

Chapter 1

Introduction

Cooperation is fundamental to human society. Some forms of cooperation support basic biological survival and reproduction, including cooperative hunting, resource sharing, collective defense against predators, and alloparental care. Others reflect uniquely human sociality, such as division of labor, gift-giving, exchange, knowledge transmission, and formation of alliances. The prosperity of *Homo sapiens* would have been impossible without these behaviors. However, the evolutionary origins of cooperation are not fully understood and have been actively studied from Darwin’s era to the present day.

While numerous factors that promote cooperation have been proposed, this dissertation focuses on environmental variability (EV) as a potentially crucial yet understudied driver. This chapter reviews the literature on the evolution of cooperation, explains why we focus on EV, outlines the research objectives and approach, and provides an overview of the dissertation’s structure.

1.1 Theoretical background

Darwin’s theory of natural selection in *On the Origin of Species* (1859) [1] includes the principle that nature favors traits that increase individual fitness—the ability for individuals to survive and reproduce. However, although cooperative behaviors, particularly altruistic ones, appear to enhance the fitness of others or the group rather than the actor’s own fitness, such behaviors are widespread across diverse taxa, from microorganisms to social insects to mammals. If natural selection favors traits that increase individual fitness and cooperation appears to decrease individual fitness, why is cooperation so ubiquitous? Darwin himself recognized this paradox [2].

This puzzle was initially studied within evolutionary biology and was later taken up by a wide range of disciplines, including physics, economics, and psychology, eventually giving rise to an interdisciplinary field known as *the evolution of cooperation*. The following paragraphs review several key studies in the evolution of cooperation, highlighting their main contributions

and limitations.

Hamilton (1964) [3, 4] introduced the concept of inclusive fitness to explain the evolution of altruistic behaviors among genetically related individuals and formalized this insight as Hamilton’s rule. This theoretical framework provides a powerful explanatory principle for cooperation among kin across diverse taxa, from social insects to primates. However, Hamilton’s rule, in its original form, cannot explain altruistic behaviors between non-relatives, which are particularly prevalent in human societies. Recent attempts have been made to extend Hamilton’s rule to general cooperation mechanisms beyond kin relationships, but the validity of these extensions remains debated [5–7].

Maynard Smith and Price (1973) [8] introduced evolutionary game theory, providing a mathematical framework for analyzing how behavioral strategies, including cooperation and defection, spread in populations. Their approach treats strategies as heritable traits subject to natural selection, allowing researchers to predict which strategies will persist in populations over evolutionary time. This framework has become fundamental to studying the evolution of cooperation, as it enables formal analysis of how cooperative and selfish strategies compete and coexist.

Axelrod and Hamilton (1981) [9] demonstrated that reciprocal cooperation can evolve among non-relatives through repeated interactions. Using the iterated prisoner’s dilemma game, they showed that simple reciprocal strategies such as Tit-for-Tat, which cooperates initially and then mimics the opponent’s previous action, can be evolutionarily successful when individuals interact repeatedly and can recognize their past partners. This work established direct reciprocity as a fundamental mechanism for the evolution of cooperation. However, this mechanism requires individuals to recognize each other and remember past interactions, making it applicable primarily to small groups with repeated encounters. In large-scale societies where interactions are often anonymous or infrequent, alternative mechanisms are needed to explain the prevalence of cooperation.

Addressing these limitations, Nowak and his collaborators advanced research on various mechanisms that promote cooperation, including indirect reciprocity [10, 11], network reciprocity [12], and group selection [13]. Building on these studies, Nowak (2006) [14] synthesized the theoretical developments in the field, proposing five fundamental mechanisms for the evolution of cooperation: kin selection, direct reciprocity, indirect reciprocity, network reciprocity, and group selection. This framework provided a comprehensive taxonomy for understanding how cooperation can evolve under different ecological and social conditions. However, Nowak’s synthesis has been criticized as essentially reformulating Hamilton’s rule in different contexts, as each of these mechanisms can be understood within the framework of inclusive fitness theory [15]. Moreover, while this taxonomy is useful for categorizing mechanisms, it does not address how these mechanisms interact or which conditions favor one mechanism over another in realistic ecological settings.

These theoretical developments have established fundamental frameworks for understanding cooperation. We can no longer naively say that cooperation is a mystery. However, these frameworks remain highly general and abstract. In recent years, research has increasingly shifted toward examining cooperation under more specific circumstances and mechanisms [16–21]. These studies investigate how factors such as reputation, social norms, memory, complex network structures, learning mechanisms, and EV shape the evolution of cooperation. Such context-specific approaches complement the general theoretical frameworks and provide insights into the diverse forms of cooperation observed in nature and human societies.

Among these context-dependent factors, we focus on EV for two reasons. First, there is a hypothesis supported by empirical data suggesting that EV drove the evolution of uniquely human behaviors (*modern human behavior*), including cooperative behavior. However, the direct causal relationship between EV and cooperation remains unclear. Second, other factors such as networks, norms, and learning algorithms are actively researched because they directly influence cooperation. However, EV appears to be less directly related to cooperation, and thus has been studied less than other factors in the field of the evolution of cooperation. These two points are detailed in the following Sections 1.2 and 1.3.

1.2 Environmental variability and the evolution of modern human behavior

Modern human behavior refers to a suite of traits characteristic of *Homo sapiens*, including abstract thinking, symbolic expression, complex planning, language, art, and crucially, large-scale cooperation and ultrasociality. Numerous studies concur that these behavioral patterns emerged during the Middle Stone Age (MSA) in Africa [22–26]. While there is broad consensus on when and where these behaviors originated, the mechanisms driving their emergence remain enigmatic despite various proposed theories.

Among various hypotheses proposed to explain these developments, the variability selection hypothesis (VSH), proposed by Potts (1996, 1998) [27, 28], suggests that EV was a primary driving force in human evolution. According to this hypothesis, intensified environmental fluctuations during MSA in Africa favored “versatilists”, those capable of rapid adaptation to new environments over “specialists”, who adapt to specific environments, or “generalists”, who adapt across a range of environments. In this context, EV encompasses changes in landscape dynamics (such as land-lake oscillations), climate fluctuations (such as arid-moist climate oscillations), variations in flora and fauna, ultimately leading to the unpredictability of resource availability.

Initially, this hypothesis was supported by a temporal correlation between intensified environmental changes, the replacement of human species, and the increased complexity of cultural

artifacts, such as stone tools and ornaments [29]. In addition, the cognitive buffer hypothesis (CBH) [30–32] provides a neuroscientific basis for VSH, and a mathematical model [33] demonstrates its theoretical feasibility. The CBH posits that larger brain sizes in animals, including humans, evolved as a buffer against EV, enhancing survival through improved problem-solving and learning abilities. In contrast, several theories [34–36] propose that EV and behavioral diversity do not necessarily drive human encephalization. These theories emphasize the role of social contexts, as suggested by the social brain hypothesis (SBH) [29, 37–43], and consider other factors such as dietary influences [44, 45]. The SBH argues that human intellectual abilities evolved in response to the selection pressures of complex social environments, which required the effective management of social relationships within and between groups.

While temporal correlations between EV and the emergence of modern human behavior are evident, the causal mechanisms remain debated. In particular, the fact that large-scale complex cooperation is a component of modern human behavior raises the question of whether EV also played a role in the evolution of cooperation. This speculative link provides the first motivation of this dissertation.

1.3 Environmental variability and the evolution of cooperation

Most previous studies on the evolution of cooperation have not considered environmental factors, assuming fixed environmental conditions. Nevertheless, a small but growing number of studies have examined cooperation under EV.

These works on EV can be broadly categorized into extrinsic EV models and intrinsic EV models. Extrinsic EV can be represented through several models, including fluctuations in the population that the environment can sustain [46, 47], stochastic variations in payoff matrices or game rules [48–50], variability in learning, and information transmission mechanisms [51, 52]. Differences in resource availability have also been studied [53], though the model does not involve temporal variability but rather compares static scenarios of abundance and scarcity. Intrinsic EV, in contrast, refers to EV in which interactions in a system modify the environment, and environmental feedback in turn shapes the system’s behavior [54, 55].

While anthropogenic environmental change is increasingly critical in modern societies, such feedback effects would be negligible in the context of MSA. Therefore, we focus on extrinsic EV rather than intrinsic EV. This extrinsic EV should capture the unpredictability of resource availability, as explained in Section 1.2. Specifically, we examine how increased intensity of EV between abundant and scarce conditions affects evolutionary dynamics, rather than unidirectional shifts from abundance to scarcity or vice versa. This aspect of EV has not been previously studied, constituting our second motivation.

1.4 Research objectives and approach

Given the research gaps identified above, this dissertation addresses the following key research questions: (i) Does EV promote cooperation? and (ii) If so, how does it?

To address these research questions, we adopt a constructive approach. The constructive approach is a methodology that seeks to understand phenomena by artificially constructing systems that reproduce them and analyzing their behavior. In the context of this dissertation, we employ multi-agent simulations based on evolutionary game theory to reproduce and examine the evolutionary dynamics of cooperative behavior under EV.

We adopt this simulation-based approach for three reasons. First, directly observing evolutionary processes is infeasible because they occur over timescales far beyond experimental reach; simulations allow us to observe such dynamics within tractable timeframes. Second, simulations enable systematic manipulation of variables such as the intensity of EV, which cannot be controlled in natural situations. Third, simulations allow us to isolate causal relationships by simplifying conditions, whereas in the real world numerous confounding factors mediate the relationship between EV and cooperation.

However, this approach has inherent limitations. Because our simulations abstract away from the complexity of real systems, they cannot provide precise quantitative predictions, such as the specific magnitude of EV required to produce a given level of cooperation. Rather, our objective is to reproduce broad qualitative patterns and to identify the mechanisms through which EV can promote or hinder cooperation, providing theoretical insights that complement empirical research.

1.5 Organization

In this chapter, we reviewed the field of the evolution of cooperation, highlighting that while general theoretical frameworks have been well established, research examining cooperation under specific contexts remains an active area of investigation. We then identified the relationship between cooperation and EV as the central focus of this dissertation and posed two research questions: whether EV promotes cooperation, and if so, how. Finally, we introduced our simulation-based constructive approach to address these questions and clarified its scope and limitations.

Numerous approaches to modeling the evolution of cooperation under EV are conceivable. In this dissertation, we consider three abstract models, examined in Chapters 2, 3, and 4. Given this diversity of possible approaches, these models are not exhaustive, yet they provide an important starting point for future theoretical and empirical research.

Chapter 2 ([The base model](#)) introduces a base model that examines the evolution of cooperation among geographically distinct groups under EV. In this model, groups represent sites at

which resources may concentrate, such as riverbanks or lakeshores, where human populations naturally gathered. A limitation of this model is that it does not account for migration between groups.

Chapter 3 ([The 2-level model with migration](#)) extends the base model by introducing a two-level structure with individual-level migration. Here, each geographical group, as defined in Chapter 2, contains multiple individuals who can move between groups. This framework allows us to examine how EV influences cooperation when individual migration is considered. However, while this model is a natural extension of Chapter 2, it represents a relatively unique approach within the existing studies on cooperation and migration, limiting comparability with prior works.

Chapter 4 ([The 2-dimensional model with migration](#)) addresses this limitation by employing a two-dimensional spatial structure, widely used in the literature on cooperation with migration. In this model, without assuming explicit group structures, as defined in Chapters 2 and 3, we investigate how EV influences cooperation among individuals moving across a two-dimensional space.

Chapter 5 ([Conclusion](#)) synthesizes the findings from the three models in Chapters 2, 3, and 4 to discuss the commonalities and differences in the mechanisms. We further consider the implications and significance of this research, as well as its limitations and directions for future work.

Finally, to provide an overall perspective, Table 1.1 summarizes the key concepts used throughout this dissertation, although some are formally described in later chapters.

Table 1.1: Key concepts used throughout this dissertation

Term	Description
Agent	An autonomous unit in simulation models that possesses a behavioral strategy, perceives its environment and takes actions. In Chapter 2, agents represent groups. In Chapter 3, two levels of agents exist: groups and individuals within groups. In Chapter 4, agents represent individuals.
Individual	An agent representing the unit of migration. Due to this definition, individuals are not necessarily single persons but may represent small units such as families. Individuals are modeled as agents in Chapters 3 and 4, but not in Chapter 2.
Group	A collection of individuals sharing a common geographical location. Groups are modeled as agents in Chapters 2 and 3, but not in Chapter 4.
Cooperation	Altruistic behavior that appears to benefit other agents at a cost to an acting agent. Cooperation (C) and its alternative behavior, defection (D), are used as behavioral strategies of an agent in game-theoretic models.
Environmental Variability (EV)	Temporal fluctuations in the spatial distribution of resource availability. This dissertation focuses on extrinsic EV, which occurs independently of human activity, reflecting unpredictable climate and landscape fluctuations during the MSA in Africa. In the later chapters, EV is usually modeled through the stochastic movement of Source of Resources (SoR) , focal points of resource abundance, and the resulting shifts in resource distribution.
Migration and Mobility	Migration means spatial movement of individuals in response to resource availability or environmental conditions, while mobility means the ability to migrate. In Chapter 2, migration is not incorporated. In Chapter 3, individuals migrate between groups. In Chapter 4, individuals migrate across a 2D space.

Chapter 2

The base model

This chapter¹ introduces a base model to examine our research questions: whether and how environmental variability (EV) promotes the evolution of cooperation. Although migration is a reasonable response to EV for people during the Middle Stone Age (MSA), we exclude it here to focus on the direct effects of EV on cooperation. The combined effects of EV and migration are examined in Chapters 3 and 4.

2.1 Model

We use an agent-based simulation model within the framework of evolutionary game theory to investigate how increasing EV influences the evolution of cooperation. Given the limited availability of detailed data on EV and the spatial distribution of hominid groups during the MSA in Africa, our model adopts a highly abstracted approach, aiming to reveal the general effects of EV based on reasonable assumptions while excluding specific details. The model operates as follows: several geographically separated regions, each with varying levels of resource accessibility, experience fluctuating resource availability over time (EV). Each region hosts a single group (agent), and interactions between groups, such as resource exchanges (game) and behavioral pattern transmission (reformation), affect and adjust their relationships.

There are several points of concern when using the term “group”. First, groups within the complex social environment described by the social brain hypothesis (SBH) are nested in a series of fractal-structured networks [43, 57, 58]. As a result, when smaller groups ally and cooperate to form a larger group, whether this cooperation is viewed as intragroup cooperation within the larger group or intergroup cooperation among the smaller groups depends on the level of analysis. For simplicity, we assume a certain level of grouping and analyze their intergroup cooperation, though this could alternatively be seen as intragroup cooperation from the perspective of a higher-level group. Furthermore, while treating groups as units of adaptation is highly debated in evolutionary biology [59–61], our focus here is on cultural evolution rather

¹This chapter is based on Inaba and Akiyama (2025) [56], published in *PLOS Complex Systems*.

than biological evolution. In this cultural context, we assume that a group has a degree of autonomy, treating individual relationships and nested group structures as a black box. Here, autonomy suggests that the basic behavioral patterns for a group regarding which groups it cooperates with or does not are influenced by intergroup interactions and evolve over time.

Agent and structure

In this chapter, each agent represents a single group and has a strategy of either cooperation or defection (“C” represents a cooperation strategy or a cooperator, while “D” represents a defection strategy or a defector). Initially, all agents are set to D, as intergroup cooperation is considered extremely unlikely [62, 63]. This chapter focuses exclusively on intergroup interactions and does not consider intragroup interactions. While a two-level model would be necessary to analyze the tension between intergroup and intragroup interactions, as seen in multilevel selection studies, a one-level model is suitable here given our focus on intergroup interactions. All agents are situated within a geographic structure, forming an interaction structure.

The geographic structure is modeled as a line segment with periodic boundary conditions, represented visually as a circle (Fig 2.1). N agents are evenly spaced along the circle. Although the one-dimensional spatial structure is used for simplicity, more realistic structures can be explored as empirical studies progress. Migration is not considered in this chapter to keep the model simple as an initial approach. We incorporate migration in Chapters 3 and 4, as it is reasonable to assume that a group might move to a resource-rich region when its resources become scarce. However, the assumption of no migration is not entirely unrealistic, as some studies have highlighted the tendency for settlement during the MSA [64–66].

The interaction structure defines the relationships between agents, which are not limited by the geographic arrangement. These relationships affect the frequency of games (described later) and are subject to rewiring through reformations (also described later). The network, where agents are represented as nodes and relationships as edges, is characterized as an undirected, unweighted, and dynamic graph. The initial network is a regular network with a degree of $k = 4$.

EV

The resource represents the amount of goods or wealth necessary for survival that a group (agent) can obtain from the natural environment (e.g., food, materials for stone tools required to gather food). Resources are allocated to each agent at each time step, with the amount varying across different regions. The node with the highest resource allocation is referred to as the *Source of Resources* (SoR). The further an agent is located from the SoR geographically, the less resource it receives, as determined by the resource decrement factor, f_{RD} . Specifically,

the resource allocated to agent i is calculated as $r_i = r_p - |i - p|f_{RD}$. Here, r_i represents the resource allocated to agent i , p is the index of the SoR, and $|i - p|$ represents the distance between i and p , accounting for the boundary conditions, rather than the usual absolute value. Additionally, there is a universal resource threshold, θ , for all agents; any agent falling below this threshold must reformulate its strategy and relationships.

In this dissertation, EV refers to resource variability, represented by stochastic models. EV can be divided into variability in distribution of resources among regions and in total quantity of resources across all regions. Although variations in resource types are also an important consideration, we simplify the model assuming a single resource type. The two forms of variability are termed regional variability (RV) and universal variability (UV). RV is a type of EV in which the distribution of resource-rich and resource-poor regions changes over time; specifically, the SoR moves randomly. The SoR's index p_t at time t fluctuates according to a stochastic process expressed as $p_{t+1} = (p_t + \Delta_t) \bmod N$. Here, Δ_t is a random integer step uniformly distributed within the range $[-\sigma_R, \sigma_R]$, where $0 \leq \sigma_R \leq N/2$. This implies that the entire resource distribution shifts geographically in tandem with the movement of the SoR. UV represents another form of EV in which the total resource quantity fluctuates randomly over time, while the resource distribution between regions remains fixed. This variability reflects large-scale fluctuations in resource availability across a wide area encompassing all regions. However, to simplify the implementation, we fix the resource values and instead model UV by varying the threshold value θ , which determines when reformation occurs. The fluctuation is modeled by a first-order autoregressive process, or AR(1) [67–69], $\theta_{t+1} = \mu_\theta(1 - \beta) + \theta_t\beta + \epsilon$ with $0 \leq \beta < 1$ and $\epsilon \sim N(0, \sigma_\theta^2)$, where μ_θ is the expected value of θ , β is the autoregressive coefficient, and ϵ is a normally distributed noise term with mean 0 and standard deviation (SD) σ_θ . The intensity of RV is determined by the shift range of the SoR (σ_R), while the intensity of UV is influenced by the autoregressive coefficient (β) and the SD of the noise term (σ_θ). We examine the impact of EV on the evolution of cooperation under three scenarios: RV, UV, and combined variability (CV), where both the SoR shifts and the threshold θ fluctuates.

Game

Communication over resources (such as primitive bartering, giving, looting) between agents is represented by simple pairwise games. These games can only be played with an opponent who is connected through a network edge. The probability that agent i selects agent j as its game opponent from its neighbors is $p_{i,j}^G = \frac{1}{n}$; n is the number of neighbors of i , and neighbors refer to agents directly connected to i in the interaction structure network. The game procedure follows a pairwise public goods game (PGG) [70–73] with resource threshold considerations. First, assume that agent i selects agent j . If the agent is C, it contributes a surplus resource $M_i = \max(r_i - \theta, 0)$. If the agent is D, it does not contribute any resource. The contributed

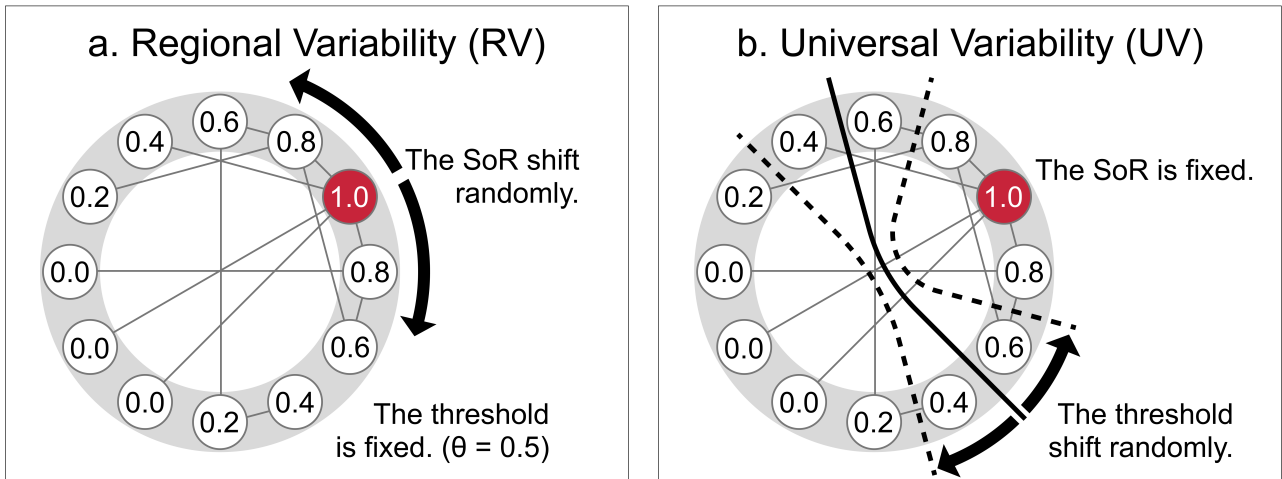


Figure 2.1: Relationships, geographical structure, and EV. Each small circle within the gray circle represents a group (agent, node), with the number inside indicating the resource value. The gray ring represents the geographical structure, and each line connecting agents denotes a relationship (edge). (a) In the RV model, the SoR shifts randomly within the geographical structure, and resources are then allocated to other nodes. Following this, the game and reformation processes occur. The resource threshold for reformation is fixed at $\theta = 0.5$. (b) In the UV model, the SoR remains fixed, but the threshold θ fluctuates randomly, following an AR(1) process.

resources are multiplied by a factor b ($1 \leq b \leq 2$) and then equally divided between i and j . The payoff table is as follows:

	C	D	
C	R_i, R_j	S_i, T_j	(2.1)
D	T_i, S_j	P_i, P_j	

$$R_i = \left(\frac{b}{2} - 1 \right) M_i + \frac{b}{2} M_j \quad (2.2)$$

$$S_i = \left(\frac{b}{2} - 1 \right) M_i \quad (2.3)$$

$$T_i = \frac{b}{2} M_j \quad (2.4)$$

$$P_i = 0 \quad (2.5)$$

The social optimum, which maximizes the sum of both payoffs, is CC under $b > 1$. The Nash equilibrium is DD when $b < 2$. Thus, a social dilemma exists across the defined range of b , except at the boundaries. Additionally, by solving $T_i > R_i > P_i > S_i$, the condition for the game to qualify as a prisoner's dilemma is $b > 1 + \frac{M_i - M_j}{M_i + M_j}$. If this condition is not met, then $T_i > P_i > R_i > S_i$.

We have chosen this game model instead of classic pairwise games to implement the condition that only agents with surplus resources can contribute to other agents. In classic pairwise

games, such as the prisoner’s dilemma or the snowdrift game, benefits and costs are fixed at constant values. This implies that agents would cooperate identically, regardless of resource abundance or scarcity, even under uncertain survival conditions. This assumption is inconsistent with our research context. Therefore, we have developed and adopted a novel pairwise PGG model that accounts for resource availability.

Reformation

When an agent’s resource level falls below the threshold θ as a result of the games, the agent is deemed to have failed to adapt to the environment, prompting a reformation of both its strategy and network connections. An agent i whose resource level falls below θ randomly selects a role model. The probability of agent j being selected as a role model is $p_j^R = \frac{r_j}{\sum_{k \in [1, \dots, N]} r_k}$. Agent i then imitates agent j ’s strategy, with mutation occurring with probability μ .

Additionally, agents that fall below the threshold disconnect all of their current relationships. They then randomly select the same number of new neighbors as the number of disconnections and establish new connections. The probability of agent j being selected as a new neighbor is p_j^R . In other words, agents with higher resources are more likely to be selected as both role models and new neighbors.

Note that mutation and EV are similar in that both introduce disturbances into the system. Mutation represents noise in strategy updating, whereas EV represents noise in resource levels. Mutation directly affects the internal state of agents. In contrast, EV does not directly affect agents; rather, it affects resource levels in the environment surrounding the agents, thereby indirectly influencing their behavior. For this reason, understanding how EV affects the collective behavior of agents is a more complex problem that warrants separate investigation.

Evaluation

The simulation runs for 10,000 generations, with 100 independent simulations conducted for each parameter set (Table 2.1). Resource allocation and interactions, including games and reformations, occur once per generation. The proportion of agents employing strategy C at the end of each generation (following the reformation process) is referred to as the cooperation rate. The average cooperation rate is calculated as the mean of cooperation rates averaged over both the last 5,000 generations and the 100 independent trials.

The cooperation rate in a single trial does not always reach a steady state within 10,000 generations and can fluctuate depending on the chosen evaluation window. However, the aggregate mean over the final 5,000 generations across 100 independent trials provides a robust and sufficiently converged measure to identify consistent qualitative patterns. This approach of utilizing late-stage averages to ensure statistical stability and mitigate initial transient effects is widely adopted in evolutionary simulation research.

To assess the effect of EV on the evolution of cooperation we compared the average cooperation rates across different parameters controlling RV and UV, along with other factors (Table 2.1).

Table 2.1: Model parameters used in the simulations.

Parameter	Description	Value options
N	Number of agents	100
ϕ_C^0	Initial frequency of cooperators	0
k_0	Initial degree of the interaction structure network	4
r_{max}	Max resource	1.0
f_{RD}	Resource decrement factor	0.02
σ_R	Shift range of the SoR; controlling the intensity of RV; random shift within $[-\sigma_R, \sigma_R]$ every generation	$\{0, 1, \dots, 49\}$
μ_θ	Expected value of threshold θ	0.5
β	Autoregressive coefficient of the UV; controlling the intensity of UV with σ_θ	$\{0, 0.1, \dots, 0.9\}$
σ_θ	SD of the noise term of UV; controlling the intensity of UV with β	$\{0, 0.1, 0.2\}$
b	Multiplication factor for PGG	$\{1, 1.1, \dots, 2\}$
μ	Mutation probability in strategy update	0.01

For a comparison with the other models, refer to Table A.1 in the Appendix.

2.2 Results

Effect of RV

We first examined the impact of RV in isolation, without considering UV. Specifically, in each generation, the SoR randomly shifts within the range of $[-\sigma_R, \sigma_R]$, accounting for the periodic boundary condition. The threshold θ , which universally affects the resource welfare of all agents, is fixed at 0.5.

The results (Fig 2.2a) suggest that RV can promote the evolution of cooperation. To elaborate, when the SoR is fixed ($\sigma_R = 0$), cooperation does not evolve. As variability slightly increases ($\sigma_R = 1$), the cooperation rate rises to around 10%. For $b \leq 1.7$, further increases in variability do not promote additional cooperation, although the cooperation rate remains higher than when $\sigma_R = 0$ or 1. However, for $b \geq 1.8$, greater variability further enhances cooperation.

Despite the overall positive effect of higher variability on cooperation, cooperation is not completely stable and fluctuates with temporary environmental changes. For example, when

$b = 1.8$ and $\sigma_R \in [1, 4, 16]$, the temporal transition (Fig 2.2b) shows that the cooperation rate rises and falls dramatically.

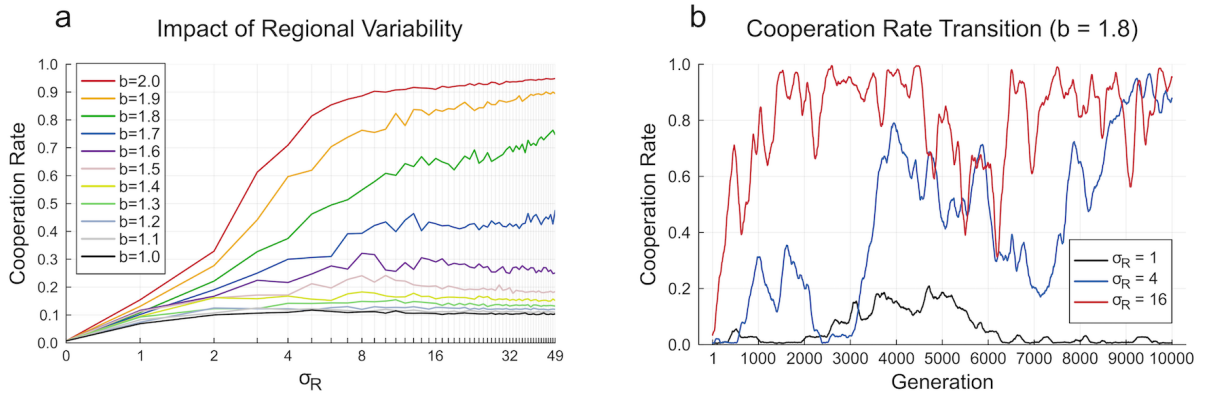


Figure 2.2: The effect of RV. (a) The effect of RV across $b \in [1.0, \dots, 2.0]$. The horizontal axis represents the intensity of RV, σ_R , and the vertical axis shows the mean cooperation rate over the last 5,000 generations, averaged across 100 trials. (b) Examples of cooperation rate transitions when $b = 1.8$ and $\sigma_R \in [1, 4, 16]$. The horizontal axis represents generations, and the vertical axis shows the cooperation rate. Higher RV tends to result in fluctuations of the cooperation rate at higher levels, though convergence is not observed.

Effect of UV

Next, we examined the effects of UV while excluding RV. As previously defined, UV refers to fluctuations in the threshold θ across generations, which uniformly affects all agents. The intensity of this variability is controlled by the autoregressive coefficient β and the SD σ_θ of the noise term in the AR(1) stochastic model. With the SoR fixed at $p = 1$, resources are allocated less as the distance from this node increases.

We found that while UV promotes the evolution of cooperation to some extent, its effect is considerably more limited than that of RV. For $\sigma_\theta = 0.1$, the cooperation rate gradually increases when β exceeds 0.5, but it peaks at just 30% (Fig 2.3a). For $\sigma_\theta = 0.2$, the cooperation rate remains between 20% and 30%, regardless of β , and increasing variability further does not affect these outcomes (Fig 2.3a).

Effect of CV

We then examined the combined effects of both RV and UV. The results (Fig 2.4) show that, consistent with the separate analyses above, RV strongly promotes the evolution of cooperation, while UV has much subtle effect.

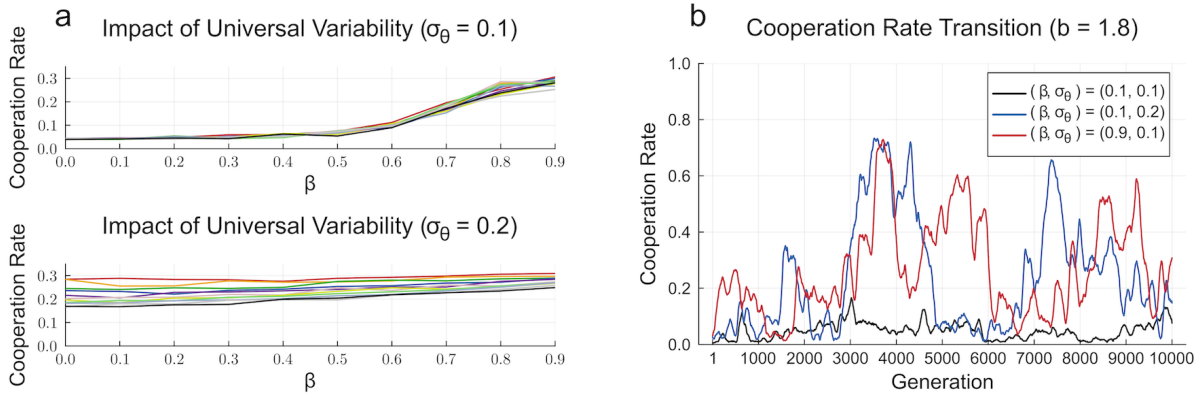


Figure 2.3: The effect of UV. (a) The effect of UV across $b \in [1.0, \dots, 2.0]$ and $\sigma_\theta \in [0.1, 0.2]$. The horizontal axis represents the intensity of UV, β , and the vertical axis shows the mean cooperation rate over the last 5,000 generations across 100 trials. (The line color scheme of these lines is same as in Fig 2.2a.) (b) Examples of the cooperation rate transition when $b = 1.8$ and $(\beta, \sigma_\theta) \in [(0.1, 0.1), (0.1, 0.2), (0.9, 0.1)]$. The horizontal axis represents generations, and the vertical axis shows the cooperation rate. Higher UV tends to result in the cooperation rate fluctuating at higher levels, but convergence is not observed.

Primary drivers of the results

The results are driven by two key factors: 1. the effects of mutation and EV, which promote fluctuations in cooperation rates, and 2. the coevolution of cooperation and network structure.

First, RV increases the fluctuations in the cooperation rate, rather than the rate itself. Fig 2.5a shows the effect of EV on strategy distribution in a model that entirely excludes the effects of games and networks. When these effects are excluded, changes in strategy distribution occur solely due to mutation and strategy updating. The Y-axis represents the number of agents generated by mutation in one generation, who then serve as role models for strategy updating in the next generation. These agents are the source of changes in strategy distribution. The line for RV in the figure shows that as the variability increases, the number of mutated role models increases linearly. Fig 2.5b “3. (env, C rate)” shows that the time series of RV and the cooperation rate in each of the 100 trials are completely uncorrelated. Furthermore, the results remain unchanged even when cross-correlation analysis is performed, accounting for time delays. Therefore, it is evident that RV does not directly affect the cooperation rate but instead promote fluctuations in it. This can be explained as follows: agents in poorer regions frequently undergo reformations and mutations. When RV is small, agents rarely accumulate resources in the next generation, causing them to undergo reformations again. However, when variability is large, agents may become resource-rich in the next generation, and they potentially survive to influence the strategy updates of other agents. When RV is large, the cooperation rate is more likely to fluctuate up and down.

Notably, the analytical solution (2.6) aligns closely with the simulation results for RV shown

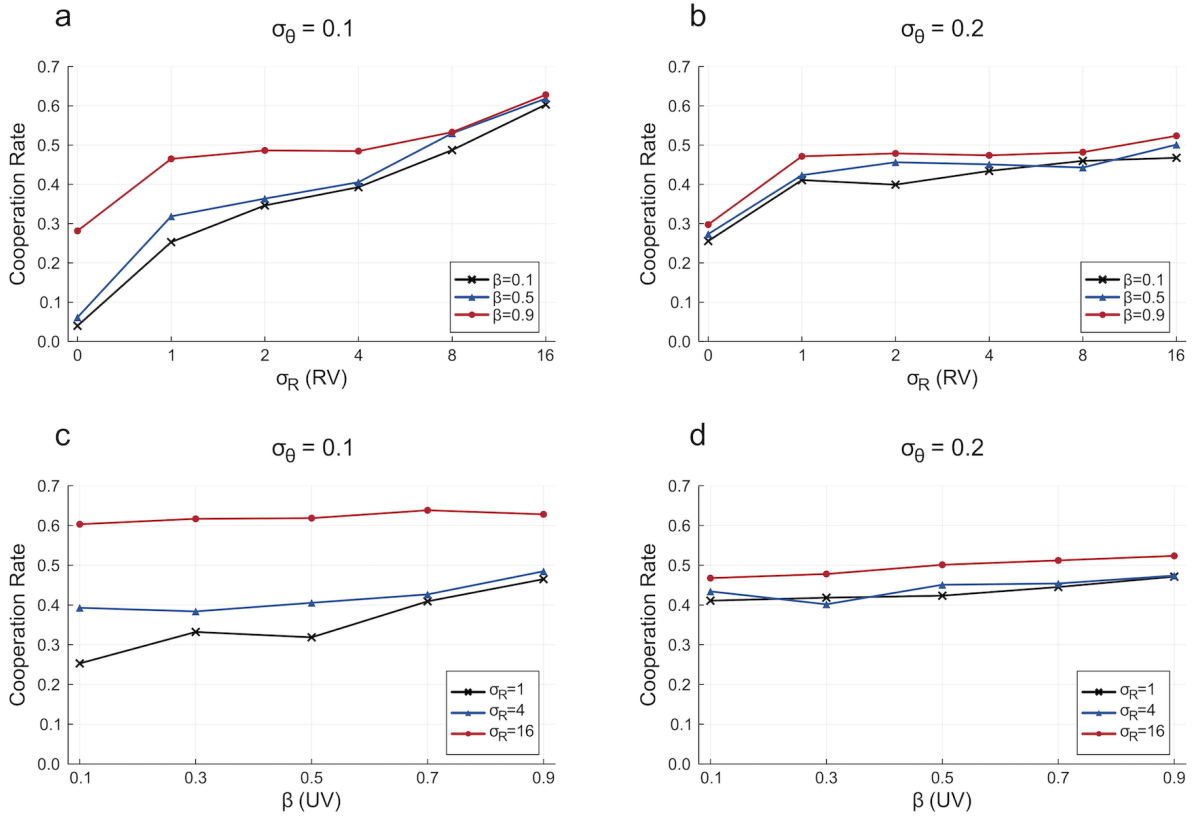


Figure 2.4: The effect of CV ($b = 1.8$). (a) and (b) represent cases with $\sigma_\theta = 0.1$, each with a different x-axis. These plots show that RV increases the cooperation rate significantly, while UV has a limited effect. (c) and (d) represent cases with $\sigma_\theta = 0.2$, with different x-axis. The lines are almost flat except in the range $\sigma_R = 0$ to 1, indicating that when UV is too high, not only UV but even RV has no effect on the cooperation rate.

in Fig 2.5a.

$$\begin{aligned} E[n_{MR}] &= \sum_{k=0}^n \mu^k (1-\mu)^{n-k} k \frac{\sigma_R}{N} \\ &= \frac{n\mu}{N} \sigma_R \end{aligned} \quad (2.6)$$

In this equation, $E[n_{MR}]$ denotes the expected number of mutated role models, which are generated through mutation and later serve as role models for the strategy updates of other agents. The right-hand side of the equation represents the expected number of mutated agents within a population of reformed agents, n , weighted by the effect of RV, σ_R , across the entire agent population, N . This equation is simplified by applying the formula for the expectation of a binomial distribution.

Second, once the cooperation rate increases, it is likely sustained through the coevolution of cooperation and network structure. Fig 2.5b 7 indicates that the cooperation rate is correlated with the difference in resources between C and D. This correlation likely arises because, as the frequency of C increases, mutual support among Cs strengthens, leading to an increase in the

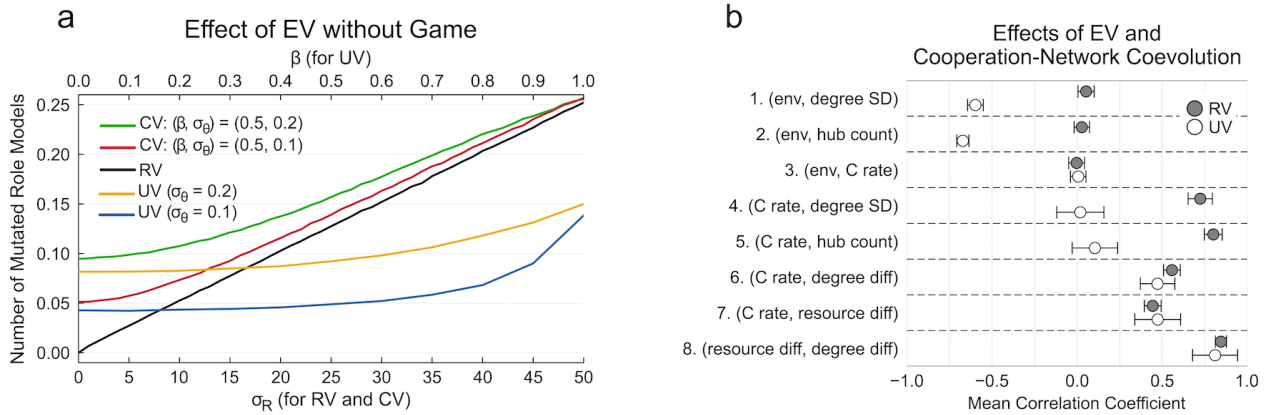


Figure 2.5: Effects of EV on Cooperation. (a) The number of mutated role models as a function of RV and UV. The simulations are based on a model that excludes games. Therefore, the figure shows how EV and reformation impact the system without the effect of games or network structure. (b) Correlation analysis through time series (10,000 generations) between variables related to EV (For RV, env refers to the shift distance of the SoR per generation; for UV, env refers to the value of threshold θ), network structure (degree SD: standard deviation of degrees, hub count: number of nodes with a degree of 10 or more), and cooperation (C rate: frequency of C, resource diff: the difference in average resources between C and D, and degree diff: the difference in average degree between C and D). The mean correlation coefficients are averaged over 100 trials for both RV and UV. $b = 1.8$ for all simulations, $\sigma_R = 16$ for RV, and $\beta = 0.7$, $\sigma_\theta = 0.1$ for UV.

average resources of C. Fig 2.5b 8 further shows that the difference in resources is strongly correlated with the difference in network degree between C and D. This occurs because, in the reformation process of our model, agents with more resources acquire more edges. Finally, Fig 2.5b 6 demonstrates that there is a correlation between the difference in degree and the cooperation rate. This is likely because, as shown in several studies [73–75], heterogeneous degree distributions tend to facilitate cooperation in networks. Thus, a positive feedback loop can form, in which an increase in the cooperation rate induces resource heterogeneity, which subsequently results in network degree heterogeneity, and this network heterogeneity, in turn, reinforces the cooperation rate, which is thought to help sustain the maintenance of a cooperation rate that initially emerged by chance. This explanation is based on correlation and inference, and does not rule out the involvement of other factors. One possible factor is the influence of resource heterogeneity on strategy update frequency, which has been suggested to promote cooperation [76]. This process may operate alongside the previously described process where an increase in the cooperation rate widens the resource gap between C and D.

In contrast, UV does not significantly promote cooperation for two reasons: it fails to generate sufficient fluctuation in the cooperation rate, and it inhibits the coevolution of cooperation and the network structure. As shown by the two UV lines in Fig 2.5a, increasing variability does not substantially increase the number of mutated role models, unlike the linear relationship seen with RV. Furthermore, when UV is intense and the threshold θ becomes very large,

almost all agents undergo reformation. This leads to a reduction in network heterogeneity, which is critical for the coevolution of cooperation and network structure. This is reflected by the strong inverse correlation between UV and network heterogeneity (Fig 2.5b 1-2). The factors that promote cooperation in RV are ineffective in the context of UV, which explains why UV does not significantly promote cooperation. When RV and UV are combined in the CV model, the results remain consistent, RV promotes cooperation, while UV has a much smaller effect.

In summary, the observed patterns in cooperation rates can be attributed to the combined effects of mutation and EV, as well as the coevolution of cooperation and network structure. Specifically, when these two factors work well together, as in the RV model, environmental change promotes cooperation. However, when the first factor is weak and inhibits the second, as in the UV model, cooperation is less likely to evolve.

2.3 Summary

This chapter models geographically separated groups arranged on a 1-dimensional circular structure without migration. Migration, a critical adaptive response to EV during the MSA, is intentionally excluded to isolate the direct effects of EV. Here, agents are defined as geographically separated regional groups. EV is implemented through three specific forms of resource variability: RV, involving the spatial shifting of the SoR, UV, involving global fluctuations in the resource threshold, and CV, combining both RV and UV. Interaction between agents is governed by a pairwise PGG, coupled with a reformation process that triggers strategy updates and network rewiring when resources fall below the resource threshold.

The results show that RV strongly promotes cooperation, UV has a marginal effect, and CV reflects the additive effects of both RV and UV. This difference arises from two key factors: the fluctuations in strategy distribution generated by EV, and the coevolution of cooperation and network structure. Both factors work effectively under RV, whereas neither factor operates effectively under UV due to insufficient fluctuations and disrupted network heterogeneity.

These findings provide a theoretical baseline for the investigations of cooperation under EV. The next chapter, Chapter 3, extends this base model by incorporating individual-level migration to examine the combined effects of EV and migration.

Chapter 3

The 2-level model with migration

While the base model in Chapter 2 demonstrated that environmental variability (EV) can promote intergroup cooperation, its exclusion of migration constitutes a significant simplification. During the Middle Stone Age (MSA), human populations likely responded to resource scarcity by migrating to more favorable environments. Therefore, this chapter introduces migration into the base model to examine how EV and migration jointly influence the evolution of cooperation.

3.1 Model

Migration can be modeled in various ways, depending on key design choices such as spatial structure, the unit of migration, migration triggers, and destination selection mechanisms.

First, regarding spatial structure, previous studies have primarily employed either patch structures [77], where agents move between discrete locations, or two-dimensional continuous spaces [78, 79], where agents move across a grid or plane. To extend the base model from Chapter 2 in a straightforward manner, this chapter adopts a patch structure where each regional group contains multiple low-level agents who can migrate between neighboring groups. The two-dimensional spatial approach is examined in Chapter 4.

Second, the unit of migration can be defined at different scales, such as individuals, families, or entire groups. In the MSA context, individual humans would rarely migrate alone due to survival constraints, and unified decision-making and simultaneous migration by large groups would be equally implausible given the complexity of group coordination. In this chapter, we do not strictly define what the unit of migration corresponds to in the real world, but conceptualize it as a small kin-based unit, such as a family or extended family group. For convenience, we refer to this unit of migration as an individual, even though this unit is not necessarily a single person.

Regarding migration triggers and destination selection mechanisms, individuals migrate, triggered by resource scarcity, toward resource-rich areas, as this research conceptualizes EV as fluctuations in resource availability.

These design choices result in a two-level hierarchical structure with group agents and individual agents. EV affects resource allocation at both levels. Game and strategy update occur independently at both levels. Migration occurs at the individual level between groups.

While Traulsen and Nowak (2006) [13] is widely recognized as a seminal study on the evolution of cooperation in a 2-level structure, the model presented in this chapter adopts a fundamentally different approach. Their model primarily analyzes the tension between individual-level interaction favoring defectors (D_s) and group-level interaction favoring groups with higher proportions of cooperators (C_s). In contrast, the 2-level model in this chapter is structured such that the payoff rules of the game (see Subsection [Game](#)) inherently define D_s as the advantageous strategy at both the individual and group levels. Given this structural disadvantage for C_s , the primary objective of this chapter is to investigate whether and how the interplay of EV and migration can facilitate the emergence and maintenance of cooperative behavior.

Structural overview

We consider the model composed of multiple regional groups, each inhabited by a number of humans who may migrate between the groups in response to environmental or social pressures. Within this world, the population is represented by group agents and individual agents, and their interaction (see Subsection [Game](#)) and migration (see Subsection [Migration](#)) are governed by the geographical and interaction structures (see Figure 3.1).

In this model, there are N_F individuals and N_R groups. An individual is an abstract representation of the minimal unit of human migration, such as a family. A group represents the set of individuals within a geographically dispersed human habitat.

The geographical structure constrains the positions of groups and the migration of individuals. It is defined as a circular graph, i.e., a ring structure, in which each group is connected to its two neighboring groups. These connections remain fixed throughout the simulation. The individuals are initially distributed evenly across all groups and can migrate between neighboring groups during the simulation. The migration results in uneven spatial distributions of individuals over time, and some groups can be empty.

The interaction structures constrain the selection of opponents for cooperative or competitive interactions at two levels, i.e., the group level and the individual level. There is a single group-level interaction structure in the model, while each group has its own individual-level interaction structure and no interactions occur between individuals belonging to different groups. An interaction structure is represented by a weighted, undirected, complete graph whose edge weights are dynamic while its topology remains fixed. Importantly, the geographical structure and the interaction structures are completely independent; the geographical distance between nodes does not influence the probability of their interaction or the weights of their relationships. The dynamic edge weight $w_{i,j}$ ($0 \leq w_{i,j} \leq 1$, initialized at w_0) denotes the strength of

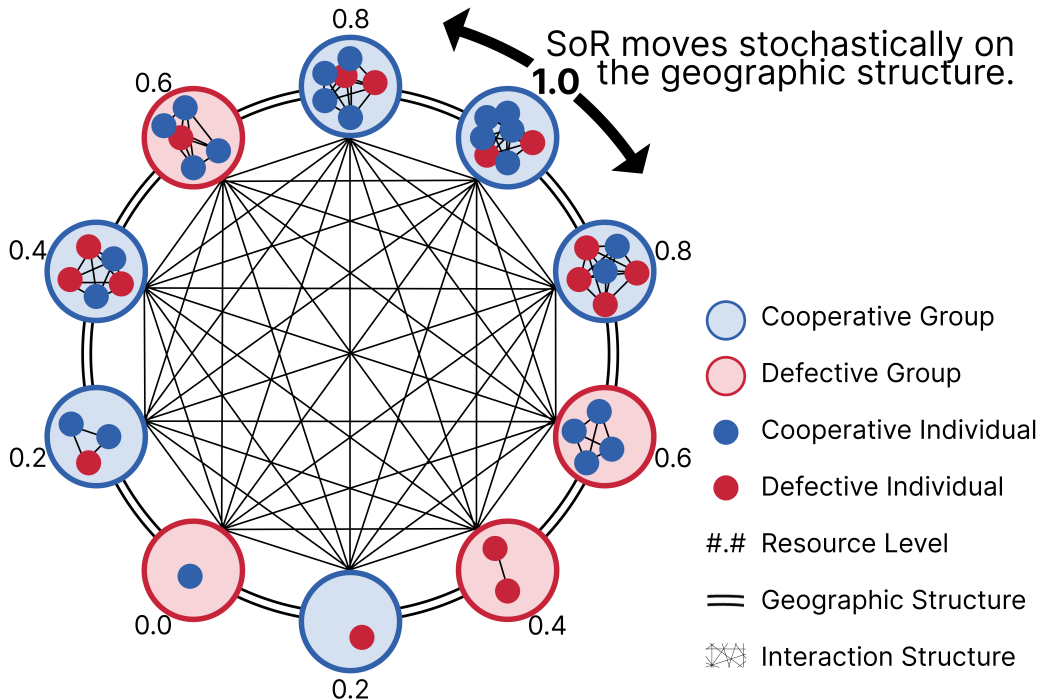


Figure 3.1: Illustration of the model structure. Regional groups are arranged on a circular geographic structure, where the SoR stochastically moves between groups. Each group contains individuals. Each group and each individual independently adopt either C (blue) or D (red). Numbers indicate group resource levels, which decrease with distance from the SoR. Interaction structures exist at the group level and at the individual level.

the relationship between nodes i and j , where a node represents either a group or an individual, and is proportional to the probability of interaction between them. In a social context, this weight represents the level of mutual trust accumulated through repeated interactions.

Given these structural foundations, the simulation proceeds in four stages: EV, game, migration, and strategy update. Game and strategy update occur at both the group and individual levels, in that order. Each stage is described in the following subsections.

Environmental variability

The model captures a key feature of the EV observed during the MSA in Africa, namely the unpredictable shifts in the geographical distribution of resources.

To represent this type of variability, we define the source of resources (SoR) as a dynamic point corresponding to the most resource-abundant region. The SoR moves stochastically across the regional groups at each simulation time step. This stochastic movement is formalized as

$$x_{t+1} = \begin{cases} [(x_t + \Delta_t - 1) \bmod N_R] + 1, & \text{with probability } p_{EV}, \\ x_t, & \text{otherwise,} \end{cases} \quad (3.1)$$

where x_t denotes the index on the circular graph of regional groups indicating the position of

the SoR at time t , $\Delta_t \in \{-1, +1\}$ is chosen with equal probability, and p_{EV} is a key parameter controlling the intensity of the EV.

The group at which the SoR is located receives a resource value of 1. The amount of resources allocated to other groups decreases with their distance from the SoR along the geographical structure, reaching 0 for the group farthest from the SoR. This resource allocation is formalized as

$$r_i^R = 1 - \frac{d_i}{\left\lfloor \frac{N_R}{2} \right\rfloor} \quad (3.2)$$

where r_i^R denotes the resources received by group i , and d_i is the distance between group i and the SoR, calculated with periodic boundary conditions. The resources of each group are evenly shared among its individuals.

Game

Interactions that affect gains and losses of resources, both between groups and between individuals, are modeled using a game-theoretic framework. For simplicity, we occasionally use the term *agent* as a general label for both group agents and individual agents throughout this chapter. Agent i adopts a strategy $s_i \in \{C, D\}$, where C denotes cooperation and D denotes defection. The interaction dynamics consist of three sequential phases: opponent selection, a pairwise public goods game (PGG), and an update of the interaction structure.

The opponent selection is based on the relationships between agents specified by the edge weights of the interaction structure. Each agent i stochastically selects another agent as its opponent, with the probability of selecting agent j given by

$$P(j|i) = \frac{w_{i,j}}{\sum_{k \neq i} w_{i,k}}. \quad (3.3)$$

Each selected pair then engages in a pairwise PGG. Here, we employ a pairwise PGG rather than traditional pairwise games such as the Prisoner's Dilemma Game and the Stag Hunt Game in order to incorporate both the resource value of each agent and the relationships into the game. This setup reflects collective activities in MSA societies at two distinct scales: individual-level games correspond to localized cooperation such as large-game hunting or commons maintenance, whereas group-level games represent broader inter-communal interactions like long-distance trade. In the game between agent i and j , both contribute their respective amounts c_i and c_j ; the total contribution is multiplied by a constant factor b , and the amplified resources are then shared equally between them. Specifically, c_i is defined as

$$c_i = \begin{cases} r_i \times w_{i,j}, & \text{if } s_i = C, \\ 0, & \text{if } s_i = D \end{cases} \quad (3.4)$$

where r_i denotes the resource available to agent i . In summary, the payoff matrix for agents i and j is

	C	D
C	$\frac{(c_i+c_j)b}{2} - c_i, \frac{(c_i+c_j)b}{2} - c_j$	$\frac{c_i b}{2} - c_i, \frac{c_j b}{2}$
D	$\frac{c_i b}{2}, \frac{c_j b}{2} - c_j$	$0, 0$

(3.5)

Finally, the edge weights of the interaction structure are updated to reflect the outcomes of the pairwise games. Because agents benefit from being connected to C but not to D , the direction of change depends on the combination of strategies [80, 81]. When $C-C$, each has an incentive to strengthen the tie, and the relationship becomes stronger. When $C-D$ or $D-C$, one side tends to strengthen while the other tends to weaken the tie; these opposing tendencies cancel out, and the relationship remains unchanged. When $D-D$, each has an incentive to weaken the tie, and the relationship becomes weaker. Formally, the update of the edge weights is given by

$$w'_{i,j} = w_{i,j} + (T - w_{i,j})\Delta w, \quad (3.6)$$

where Δw ($0 \leq \Delta w \leq 1$) denotes the update rate, and the target value T is set to 1 if $C-C$, $w_{i,j}$ if $C-D$ or $D-C$, and 0 if $D-D$.

Migration

Individuals facing resource scarcity stochastically migrate to an adjacent regional group in search of better conditions. Specifically, the probability that migration occurs is given by

$$\max\left(1 - \frac{r_i^F}{\theta_F}, 0\right) \cdot p_M, \quad (3.7)$$

where r_i^F denotes the resource available to individual i , θ_R ($0 < \theta_R < 1$) is the universal resource threshold shared by all groups, θ_F is the per-individual threshold obtained by $\theta_F = \frac{\theta_R}{N_F/N_R}$, and p_M is a parameter controlling the frequency of migration events.

The migration direction is also probabilistic: with probability p_{SoR} , the individual moves to the neighboring group closer to the SoR; otherwise, it chooses randomly between the two neighboring groups.

Upon migration, the individual establishes new relationships in the destination group, and discards all previous ones. Specifically, the edge weights between the individual and the others in the destination group are set to w_0 , and the edge weights between the individual and the others in the original group are set to 0.

Strategy update

Agents stochastically update their strategies in response to resource scarcity. Specifically, the probability that an update occurs is given by $\max\left(1 - \frac{r_i}{\theta}, 0\right) \cdot p_{SU}$, where p_{SU} is a parameter

controlling the frequency of strategy update events. An agent i that updates its strategy stochastically selects another agent j as its role model from the appropriate pool: group agents select from all other group agents, while individual agents select from other individuals within the same group. The probability of selecting agent j is given by

$$Q(j|i) = \frac{r_j}{\sum_{\substack{k \neq i \\ r_k > \theta}} r_k} \quad (3.8)$$

where θ denotes the relevant threshold, i.e., θ_R at the group level and θ_F at the individual level. The adopted strategy is then subject to mutation with probability μ , resulting in a stochastic switch between C and D . After the update, all edges of the updated agent are reset to the baseline weight w_0 . This process models success-biased cultural transmission, where agents improve survival by imitating the norms of more prosperous agents (e.g., successful hunters, thriving neighboring regions) and resetting their social ties.

Evaluation

To examine how EV and migration influence the evolution of cooperation, we conduct simulations across a range of parameter settings, as summarized in Table 3.1. For each setting, 100 independent runs of 10000 generations are carried out. As the principal performance indicators, we calculate the cooperation rates ϕ_R^C and ϕ_F^C , defined as the average proportions of groups and individuals, respectively, employing strategy C . Specifically, ϕ_R^C is the mean of the proportions of the N_R groups employing strategy C at the end of each generation (following the strategy update stage), averaged over the last 5000 generations and 100 independent runs. ϕ_F^C is calculated in the same manner, using the proportions of the N_F individuals employing strategy C .

3.2 Results

Key results: influence of environmental variability and migration

We conducted computational experiments to investigate how the EV (p_{EV}) and the migration (p_M) affect the cooperation rates at the group level (ϕ_C^R) and the individual level (ϕ_C^F).

Both ϕ_C^R and ϕ_C^F increase with p_{EV} , though with different patterns. At the group level (Figure 3.2a), ϕ_C^R values are around 0.5 at $p_{EV} = 0$, increase sharply to approximately 0.7 by $p_{EV} = 0.1$, and then increase gradually to approximately 0.8 for $p_{EV} > 0.1$. This pattern does not depend on p_M . At the individual level (Figure 3.2b), ϕ_C^F values are below 0.1 at $p_{EV} = 0$ except at $p_M = 0$; however, they increase steeply by $p_{EV} = 0.1$ and plateau at levels determined by p_M for $p_{EV} > 0.1$.

Table 3.1: Model parameters used in the simulations.

Parameter	Description	Value options
N_R	Number of group agents	{10, 20, 40, 80}
N_F	Number of individual agents	{100, 200, 400, 800, 1600, 3200, 6400}
ϕ_C^0	Initial frequency of cooperators	{0, 0.5, 1}
w_0	Initial edge weight	{0, 0.1, ..., 1}
p_{EV}	Probability of SoR shift; controlling the intensity of EV	{0, 0.1, ..., 1}
θ_R	Resource threshold at group level	0.5
b	Multiplication factor for PGG	{1, 1.1, ..., 2}
Δw	Update rate of edge weights	{0, 0.1, ..., 1}
p_M	Probability factor multiplied by resource deficit for migration events, controlling the individual mobility	{0, 0.1, ..., 1}
p_{SoR}	Probability of migrating toward SoR	{0, 0.1, ..., 1}
p_{SU}	Probability factor for strategy update events	0.1
μ	Mutation probability in strategy update	{0, 0.01, 0.05, 0.1}

For a comparison with the other models, refer to Table A.1 in the Appendix.

While p_M does not affect ϕ_C^R (Figure 3.2c), p_M significantly influences ϕ_C^F (Figure 3.2d). When $p_{EV} > 0$, ϕ_C^F is approximately 0.6 at $p_M = 0$, increases to 0.8–0.9 at $p_M = 0.1$, and then decreases linearly for $p_M > 0.1$. In contrast, when $p_{EV} = 0$, ϕ_C^F starts at approximately 0.45 at $p_M = 0$ and declines rapidly as p_M increases.

Figure 3.3 shows standard deviations corresponding to Figure 3.2. Although the mean values exhibit clear patterns (Figure 3.2), the high inter-trial variability arises because ϕ_C^R and ϕ_C^F do not stabilize over time within each individual trial, with different trials converging toward either 0 or 1.

Primary drivers of the key results

To examine the direction of influence between the group-level and individual-level processes, we conducted ablation experiments by selectively disabling specific model components. The results show that disabling individual-level games, migration, and strategy updates does not significantly affect ϕ_C^R values (compare Figure 3.2a,c to Figure 3.4a,c), whereas disabling group-level games and strategy updates markedly suppresses ϕ_C^F values (compare Figure 3.2b,d to Figure 3.4b,d). This asymmetry indicates that group-level processes contribute to individual-level cooperation, while the reverse influence is minimal.

The evolution of group-level cooperation by EV can be explained by temporal resource

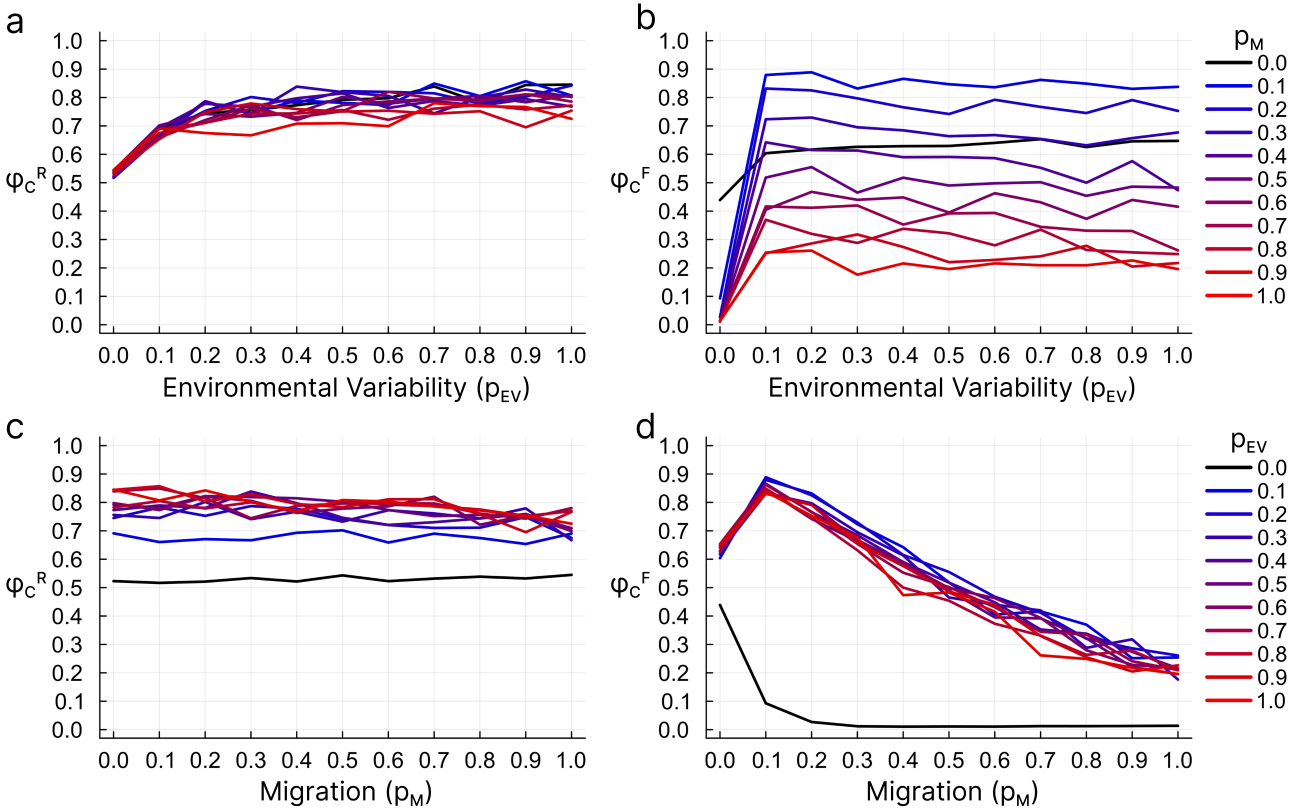


Figure 3.2: Average cooperation rates as functions of p_{EV} and p_M . (a) ϕ_C^R vs. p_{EV} for different p_M values. (b) ϕ_C^F vs. p_{EV} for different p_M values. (c) ϕ_C^R vs. p_M for different p_{EV} values. (d) ϕ_C^F vs. p_M for different p_{EV} values. Each data point represents the mean across 100 independent trials, where each trial is averaged over the final 5000 generations. Other parameters: $N_R = 10$, $N_F = 100$, $\phi_C^0 = 0.5$, $w_0 = 0.3$, $\theta_R = 0.5$, $b = 1.9$, $\Delta w = 0.1$, $p_{SoR} = 0.1$, $\mu = 0.01$.

distribution patterns (Figure 3.5).

When $p_{EV} = 0$, the resource-rich region remains fixed at group 1, creating persistent spatial inequality where groups near the SoR remain resource-rich and maintain stable strategies, while distant groups experience resource scarcity and undergo frequent strategy updates (Figure 3.5a). This spatial segregation prevents the formation of stable cooperative networks across all groups.

In contrast, when $p_{EV} > 0$, the location of the resource-rich region shifts over time, ensuring that all groups experience both resource-rich and resource-poor periods. This temporal equity increases the long-term value of maintaining cooperative relationships through group-level games. As shown in Figure 3.5c, cooperative networks gradually form and stabilize throughout the population. Groups adopting C strategies build strong reciprocal relationships, while defecting groups become isolated. These cooperative networks provide robustness against both resource fluctuations and occasional mutations.

The evolution of individual-level cooperation (Figure 3.6a) by EV can be explained by temporal resource fluctuations in a group and relationship formation between cooperators.

When $p_{EV} = 0$, the resource distribution across groups remains fixed, leading to population concentration around the resource-rich groups. Since resources are shared equally among indi-

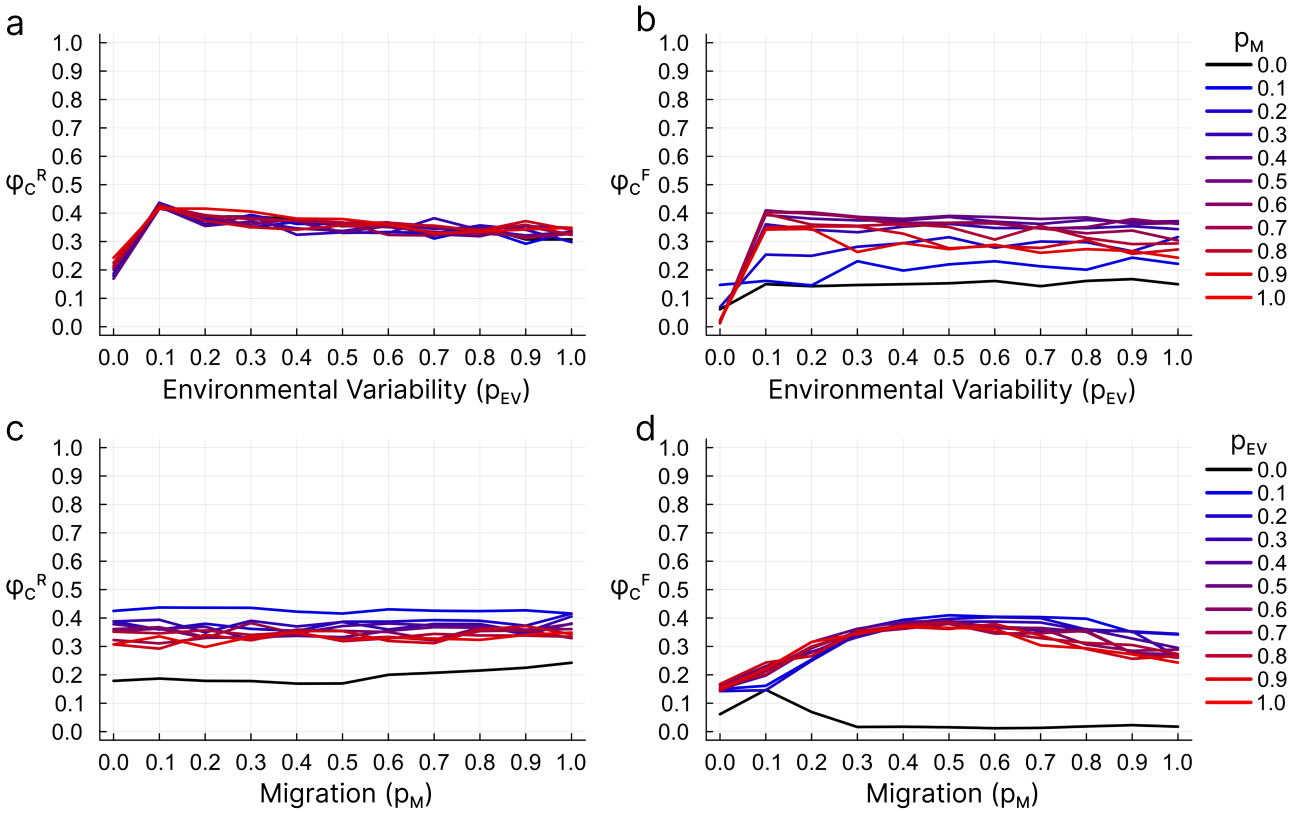


Figure 3.3: Standard deviations corresponding to Figure 3.2.

viduals within each group, this concentration equalizes per-capita resources across all groups (Figure 3.6b). In this equilibrium state, defectors outcompete cooperators due to PGG rules: cooperators invest resources while defectors receive resources without contributing (Figure 3.6c). Consequently, resource-poor cooperators undergo strategy updates and imitate high-resource defectors as role models, leading to the dominance of defectors.

In contrast, when $p_{EV} > 0$, stochastic SoR movement dynamically reshapes the resource distribution and causes previously poor groups to become rich and vice versa. Because migration requires time, disparities in per-capita resources between groups occasionally emerge after each SoR movement (Figure 3.6b). In newly enriched groups, cooperators' resources exceed the threshold, preventing both migration and strategy updates. These stable cooperators repeatedly interact with each other, gradually strengthening their mutual relationships, while defector relationships decline, isolating them from profitable interactions. Naturally, the groups can become poor. Even in that case, the strong relationships once established between cooperators enable them to maintain high resource levels through high-payoff mutual cooperation, while defectors with weak relationships remain isolated from profitable interactions. Through this process, cooperators become robust against resource fluctuations and seldom undergo migration and strategy updates, while defectors undergo migration and strategy updates more frequently (Figure 3.6c).

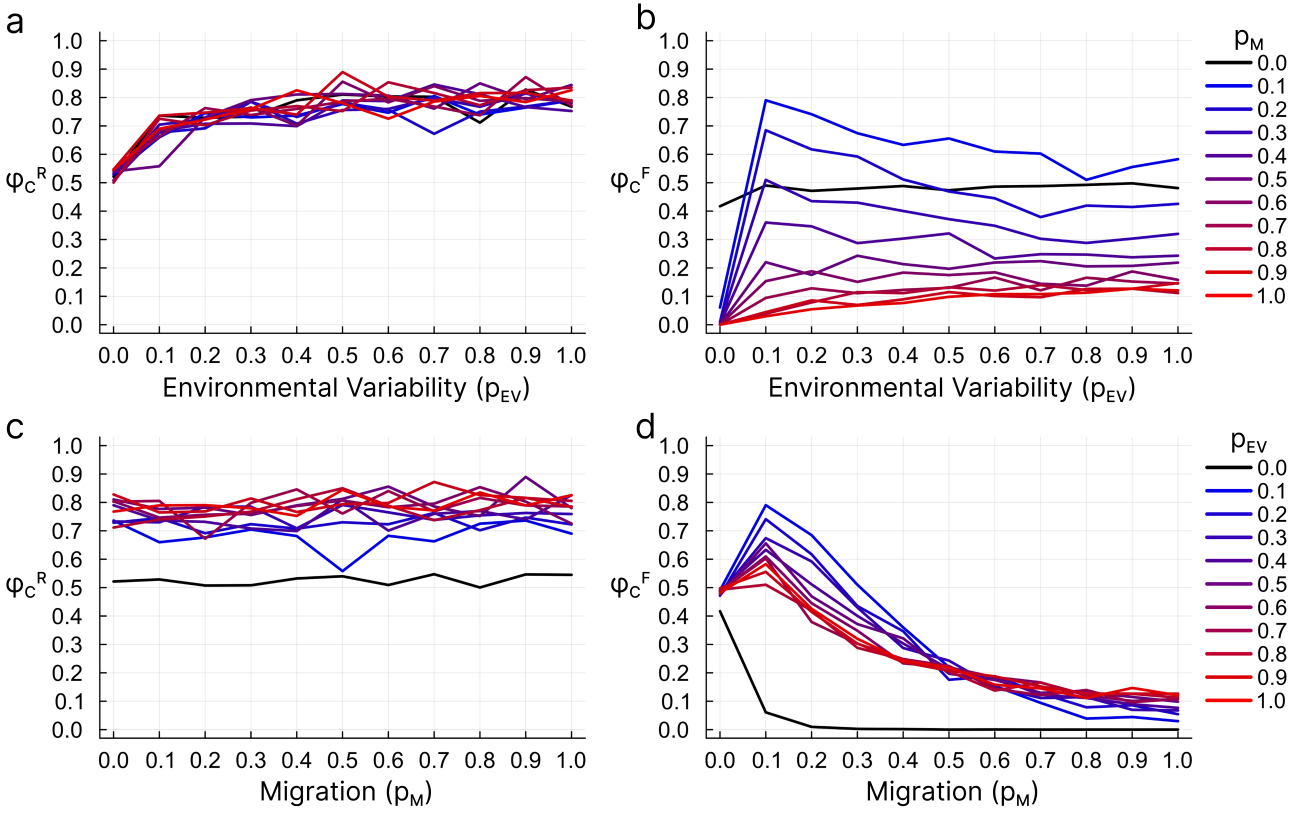


Figure 3.4: Ablation experiments corresponding to Figure 3.2. (a) and (c) show ϕ_C^R when individual-level games, migration, and strategy updates are disabled. (b) and (d) show ϕ_C^F when group-level games and strategy updates are disabled. Comparison with Figure 3.2 reveals that ϕ_C^R maintains similar patterns regardless of individual-level processes, whereas ϕ_C^F is substantially reduced without group-level processes. All other conditions are identical to Figure 3.2.

Influence of population-related parameters

Figure 3.7 shows the effects of population size parameters N_R and N_F/N_R on cooperation rates ϕ_C^R and ϕ_C^F under different environmental and migration conditions (p_{EV}, p_M). When $(p_{EV}, p_M) = (0.0, 0.0)$, both N_R and N_F/N_R have negligible effects on ϕ_C^R and ϕ_C^F (Figure 3.7a,b). When $(p_{EV}, p_M) = (0.0, 0.1)$, ϕ_C^R remains unaffected by population sizes (Figure 3.7c), whereas ϕ_C^F increases with both N_R and N_F/N_R (Figure 3.7d). When $(p_{EV}, p_M) = (0.5, 0.0)$, ϕ_C^R decreases slightly as N_F/N_R increases but remains largely unaffected by N_R (Figure 3.7e). At the individual level, ϕ_C^F decreases slightly with increasing N_R , but increases modestly with increasing N_F/N_R (Figure 3.7f). These patterns observed under $(p_{EV}, p_M) = (0.5, 0.0)$ remain essentially unchanged when $(p_{EV}, p_M) = (0.5, 0.1)$ (Figure 3.7g,h).

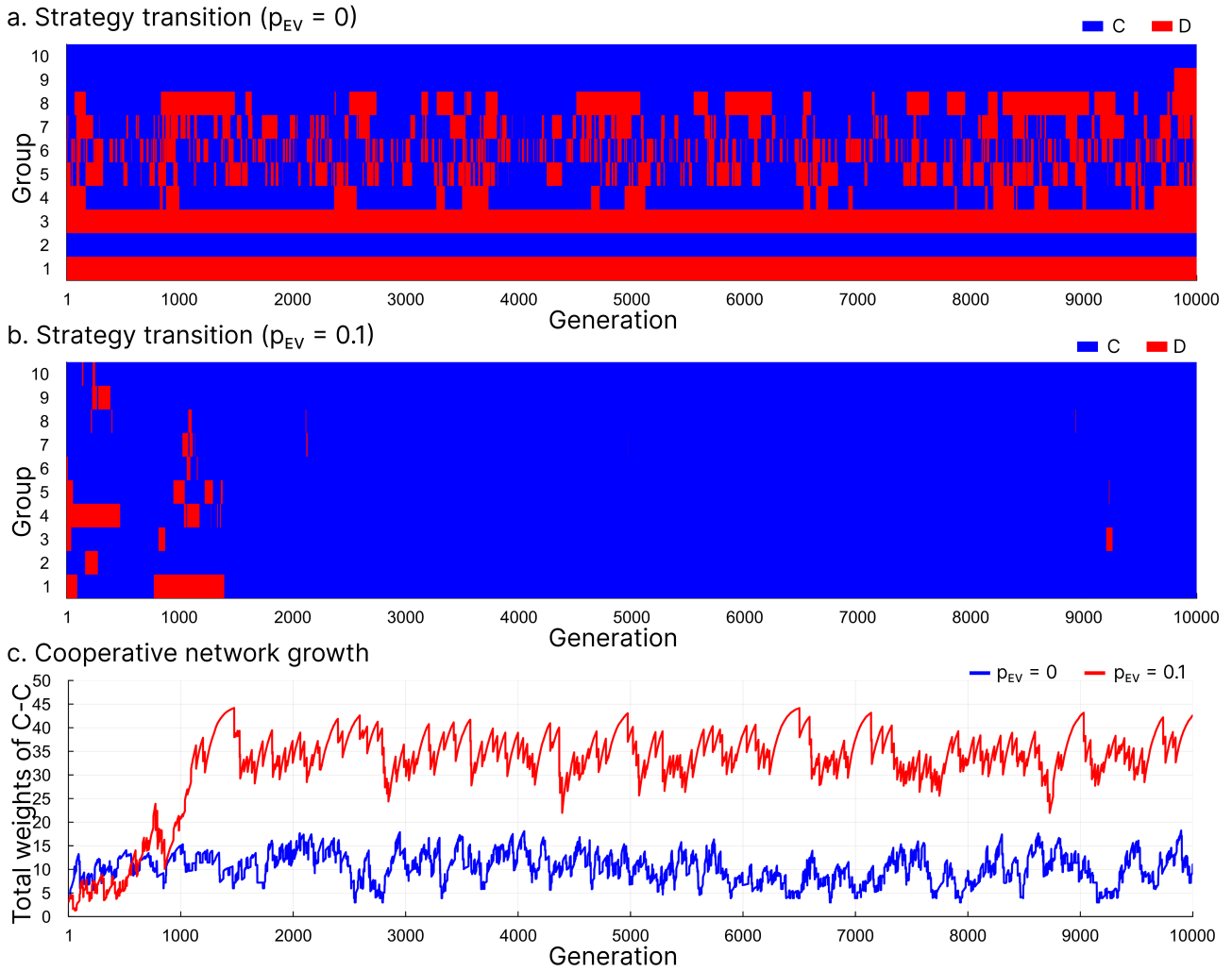


Figure 3.5: Temporal evolution of group-level cooperation. The horizontal axis represents generation, and the vertical axis represents group index. Blue indicates C and red indicates D . (a) shows the case where $p_{EV} = 0$ with the resource-rich region fixed at group 1. (b) shows the case where $p_{EV} = 0.1$ with a shifting resource-rich region. Occasional mutations introduce D , but they quickly revert to C . (c) shows the transition of the sum of weights between C and C' . All other conditions are identical to Figure 3.2.

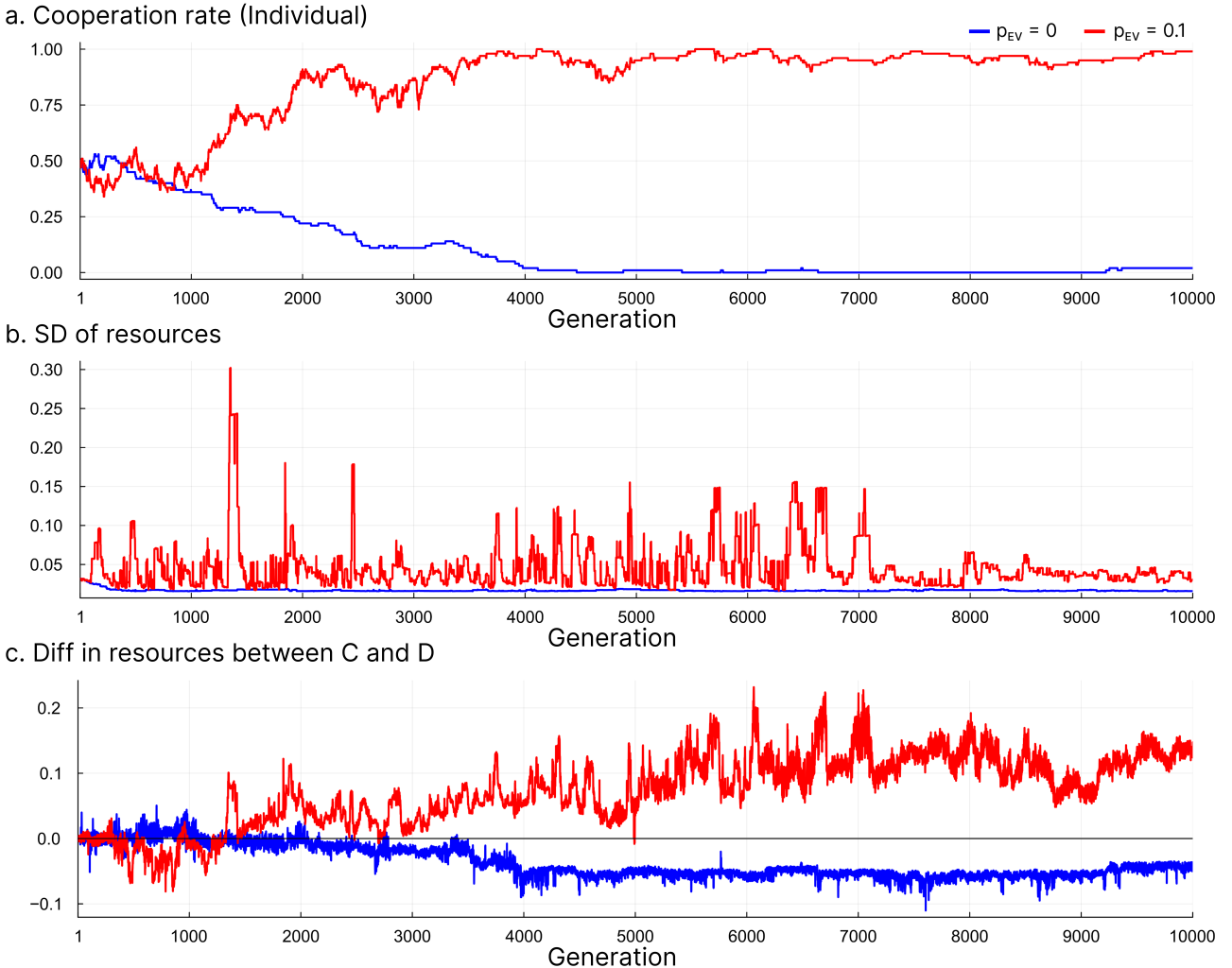


Figure 3.6: Evolution of individual-level cooperation and resource dynamics. (a) Cooperation rate at the individual level (ϕ_C^F) over time: when $p_{EV} = 0$, ϕ_C^F declines to near zero, while when $p_{EV} = 0.1$, ϕ_C^F reaches and maintains high levels. (b) Standard deviation (SD) of mean individual-level resources between groups over time: when $p_{EV} = 0$, the SD converges to near zero as resources equalize across groups, while when $p_{EV} = 0.1$, stochastic SoR movement maintains persistent fluctuations in resource disparities between groups. (c) Difference in mean resources between C and D within groups over time: when $p_{EV} = 0$, the difference remains small and negative, while when $p_{EV} = 0.1$, C consistently maintain substantially higher resources than D within the same groups. All other conditions are identical to Figure 3.2.

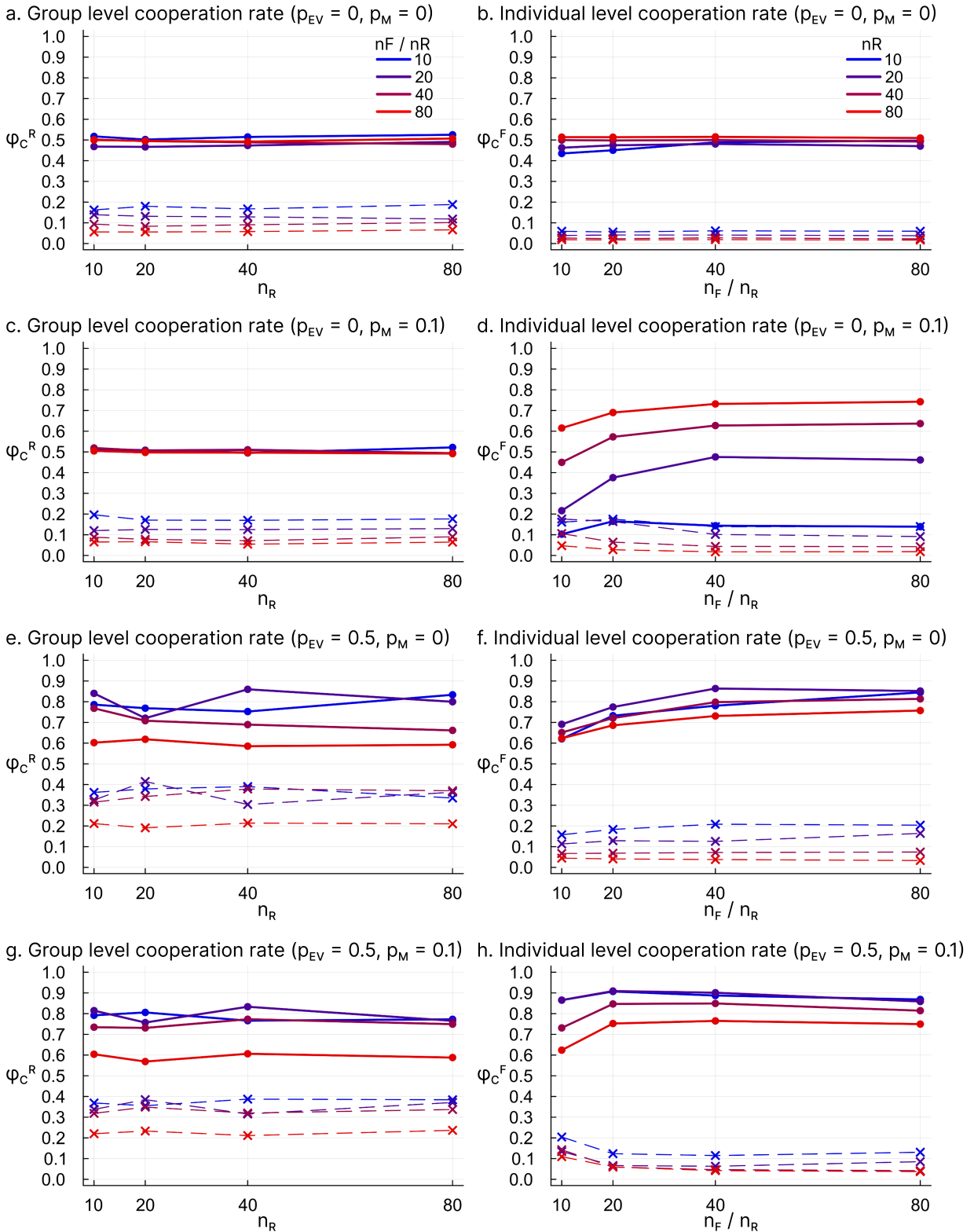


Figure 3.7: Effects of population size parameters N_R and N_F/N_R on the cooperation rates ϕ_C^R and ϕ_C^F . The left panel column (a,c,e,g) shows the group-level cooperation rates ϕ_C^R , and the right panel column (b,d,f,h) shows the individual-level cooperation rates ϕ_C^F . Each panel row corresponds to a different parameter setting of (p_{EV}, p_M) .

These patterns can be explained as follows. The group-level cooperation rate is insensitive

to population size parameters for the following reasons. Regarding N_R , because the resource allocation is normalized such that the group at the SoR receives 1.0 and the most distant group receives 0.0 regardless of the number of groups, increasing N_R does not change the range of resource values that groups experience. Regarding N_F/N_R , group-level dynamics are governed solely by intergroup relationships and EV, independently of the number of individuals within groups. At the individual level, larger N_F/N_R generally promotes cooperation because more individuals within each group increases the absolute number of cooperators even if the proportion of cooperators is the same, enabling them to form mutual relationships that are more robust against exploitation by defectors. The effect of N_R on ϕ_C^F depends on whether EV is present: without EV ($p_{EV} = 0$), increasing N_R increases the number of groups with moderate resource levels around the SoR, enabling cooperators to remain in the same group and strengthen the relationships among them. with EV ($p_{EV} > 0$), increasing N_R increases the frequency of migration, thereby limiting opportunities for cooperators to form stable networks within their groups.

The initial cooperation rate ϕ_C^0 influences the evolutionary outcomes (Figure 3.8). When $\phi_C^0 = 0$ (lower area in each panel of Figure 3.8), cooperation rates are lower overall compared to $\phi_C^0 = 0.5$ (Figure 3.2), but the qualitative patterns remain unchanged. In contrast, when $\phi_C^0 = 1$, the patterns change dramatically. Both ϕ_C^R and ϕ_C^F are approximately 1.0 when $p_{EV} = 0$ and decline as p_{EV} increases (upper area in each panel of Figure 3.8a,b). Similar patterns are observed as p_M increases (upper area in each panel of Figure 3.8c,d).

The influence of ϕ_C^0 reflects the difference between the emergence and maintenance of cooperation. When $\phi_C^0 = 0$ or 0.5, cooperation must emerge through mutation and strategy updating, which EV facilitates. In contrast, when $\phi_C^0 = 1$, cooperative networks are already established; in stable environments ($p_{EV} = 0$), these networks persist because few agents fall below the resource threshold and undergo strategy updates, whereas EV and migration can disrupt these pre-existing networks.

Influence of network parameters

The initial network weight w_0 negatively influences cooperation, with lower w_0 promoting cooperation at both levels (Figure 3.9a,b). This occurs because w_0 determines the interaction strength with newcomers introduced through migration or strategy updates. When w_0 is small, newcomers have weak initial relationships with existing members, limiting their immediate impact on the system. If a newcomer adopts D , the low w_0 prevents strong interactions that could disrupt established cooperative networks. In contrast, when w_0 is large, defecting newcomers immediately engage in strong interactions with C , potentially destabilizing the cooperative network and reducing overall cooperation rates.

The update rate of relationship weights Δw positively affects cooperation, with higher Δw

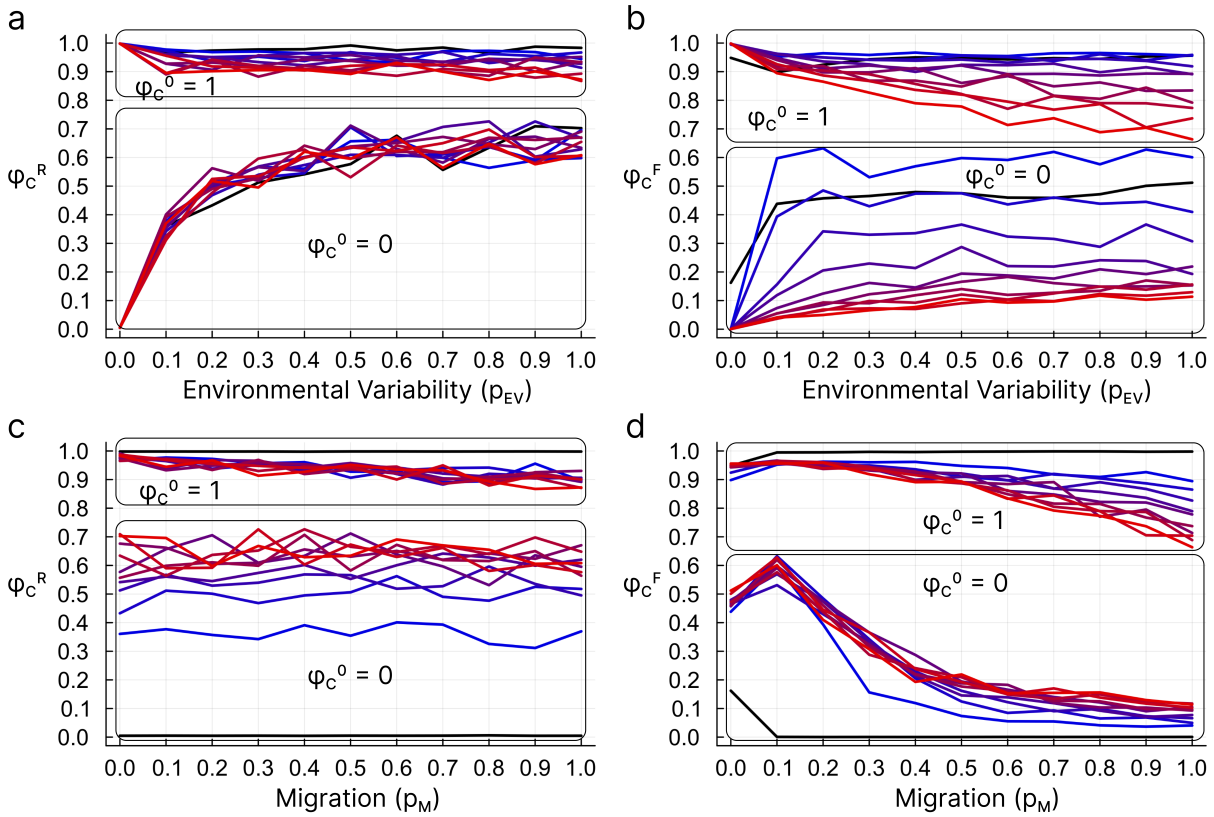


Figure 3.8: Effects of initial cooperation rate ϕ_C^0 . In each panel, the lower area shows the case where $\phi_C^0 = 0$, and the upper area shows the case where $\phi_C^0 = 1$. (a) ϕ_C^R vs. p_{EV} for different p_M values. (b) ϕ_C^F vs. p_{EV} for different p_M values. (c) ϕ_C^R vs. p_M for different p_{EV} values. (d) ϕ_C^F vs. p_M for different p_{EV} values. All other conditions and the color scheme are identical to Figure 3.2.

promoting cooperation at both levels (Figure 3.9c,d). Higher Δw values enable relationship weights between C pairs to rapidly increase and those between D pairs to quickly decline, thereby accelerating the formation of cooperative networks.

Influence of other parameters

We examined the effects of several additional parameters: the SoR orientation (p_{SoR}), the PGG multiplier (b), and the mutation rate (μ). The parameter p_{SoR} has no significant effect on cooperation rates. Higher values of b promote cooperation at both levels, as expected from standard PGG theory. Higher μ values blur the patterns observed in mean cooperation rates while reducing inter-trial variability, but do not alter the qualitative patterns. Since these results are either trivial or follow directly from model assumptions, detailed results are provided in the Appendix.

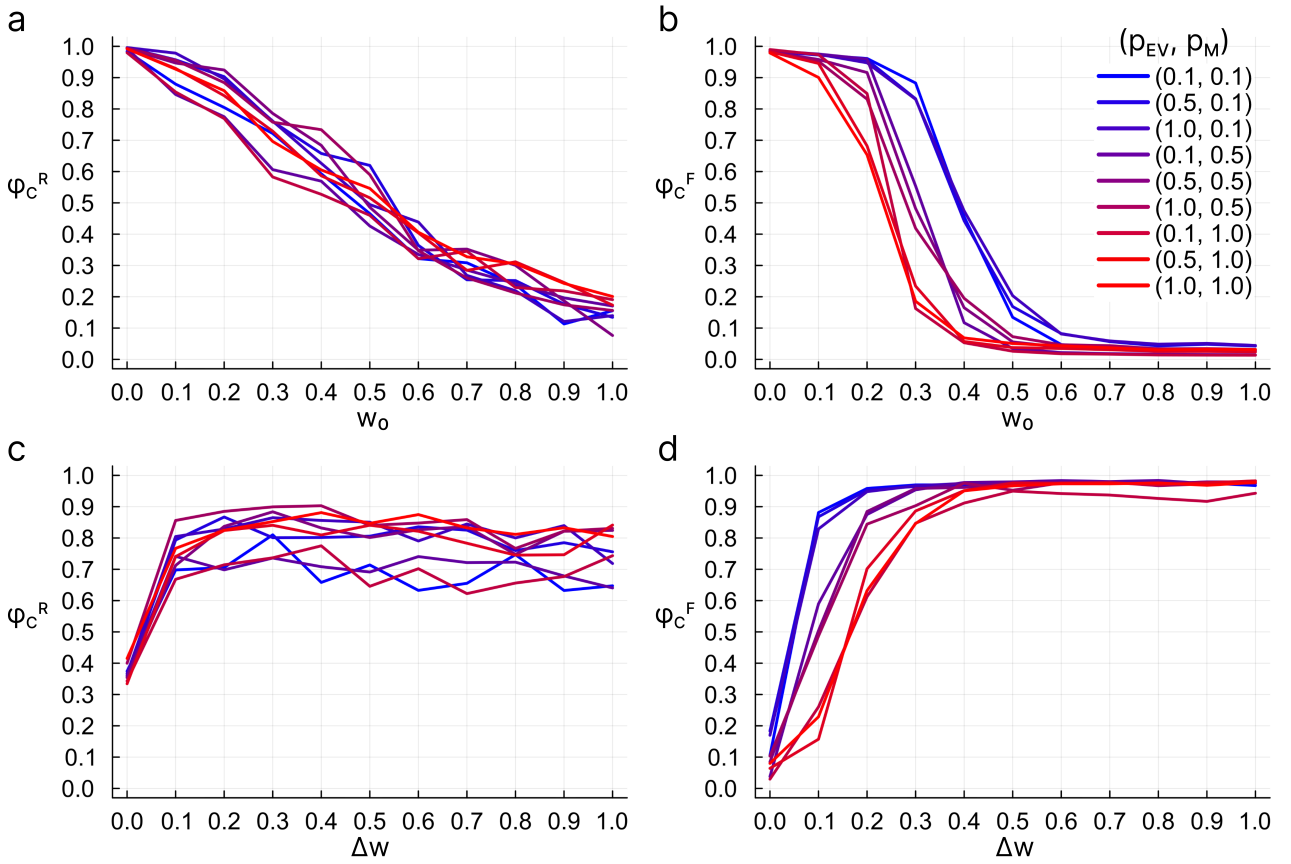


Figure 3.9: Effects of initial network weight w_0 and relation weight update rate Δw on cooperation rates ϕ_C^R and ϕ_C^F . (a) ϕ_C^R vs. w_0 for different (p_{EV}, p_M) values. (b) ϕ_C^F vs. w_0 for different (p_{EV}, p_M) values. (c) ϕ_C^R vs. Δw for different (p_{EV}, p_M) values. (d) ϕ_C^F vs. Δw for different (p_{EV}, p_M) values. All other conditions are identical to Figure 3.2.

3.3 Summary

This chapter extends the base model to investigate the joint effects of EV and migration by introducing a 2-level hierarchical structure consisting of group-level agents and individual-level agents within them. While the group agents are the same as in Chapter 2, the individual agents newly introduced in this chapter are allowed to migrate between neighboring groups in response to resource scarcity. Interactions at both group and individual levels are governed by independent weighted networks, where the weights represent the strength of relationships. Pairwise PGGs are played on both levels and the network weights are updated based on game outcomes; specifically, relationships between cooperators strengthen, while relationships involving defectors weaken or remain static.

The results demonstrate the following key findings: (i) the group-level cooperation rate gradually increases with the EV (p_{EV}); (ii) the individual-level cooperation rate sharply increases by $p_{EV} = 0.1$ and plateaus for $p_{EV} > 0.1$; (iii) unlike group-level cooperation, individual-level cooperation is strongly affected by migration: moderate migration ($p_M \approx 0.1$) maximizes cooperation, while excessive migration reduces it. At both levels, EV promotes cooperation through

the formation of cooperative networks that provide robustness against resource fluctuations, migration, and strategy updates, similar to the mechanism in the base model in Chapter 2. A detailed comparison between the models is provided in Chapter 5. In addition, lower initial relationship strength (w_0) and faster updating of relationship weights (Δw) further facilitate the formation and maintenance of cooperative networks.

These findings demonstrate that EV remains a powerful driver of cooperation even when individual mobility is incorporated. The next chapter, Chapter 4, examines the effects of EV and migration in a two-dimensional spatial structure without explicit group definitions.

Chapter 4

The 2-dimensional model with migration

In Chapters 2 and 3, we examined the evolution of cooperation under environmental variability (EV) using models with explicit group structures. The base model in Chapter 2 demonstrated that EV can promote cooperation without migration. The 2-level model with migration in Chapter 3 extended this by introducing individual-level migration and demonstrated that EV can still promote cooperation. Moreover, moderate migration promotes cooperation while excessive migration hinders it. However, the 2-level model is relatively unique and limits clear comparison with existing studies on cooperation and migration. In this chapter¹, we adopt a 2-dimensional (2D) space, which is widely used in the literature, diverging from the group-structured frameworks of Chapters 2 and 3 to prioritize comparability with prior works.

The evolution of cooperation among mobile agents has been studied actively. Dugatkin and Wilson (1991) [77] performed pioneering work in this area, demonstrating that the effectiveness of Axelrod's Tit-for-Tat strategy [9] can be undermined by mobile defectors (Rover strategy) when migration costs are low, although their model employed a patch structure rather than a 2D space. More contemporary research in 2D spatial settings, where both cooperators and defectors can migrate, was initiated by Vainstein and Arenzon (2001) [78] and established by Vainstein et al. (2007) [79]. They demonstrated that mobility can have contrasting effects: under certain conditions, it promotes cooperation by facilitating cooperator clustering and separation from defectors, while under other conditions, it hinders cooperation by generating strategic chaos. These developments are reviewed in Perc and Szolnoki (2010) [17]. Building on Vainstein's framework, various migration strategies [83–89] differing in trigger conditions and migration distance have been proposed more recently. However, to the best of our knowledge, no study has examined the effects of extrinsic EV on the evolution of cooperation among mobile agents.

This chapter addresses this gap within Vainstein's framework by modeling EV as randomly

¹This chapter is based on Inaba and Akiyama (2025) [82], published in *Chaos, Solitons & Fractals*.

moving resource-rich spots (Sources of Resources; SoRs) across a 2D space and agent mobility as resource-seeking migration. Through extensive simulations, we examine whether and how these factors jointly promote cooperation.

4.1 Model

In this chapter, we developed a multiagent simulation model to examine how agent mobility and EV jointly influence the evolution of cooperation in spatially structured populations. Due to the limited availability of archaeological data on spatial resource distributions and hominin behavioral patterns during the MSA, we adopted an abstracted approach that prioritizes the identification of fundamental mechanisms over reproducing specific historical scenarios. This model incorporates four key processes, i.e., (i) EV on a 2D lattice, (ii) pairwise game interactions, (iii) conditional agent migration driven by resource availability, and (iv) strategy updating. These processes are described in the following subsections.

Environmental variability

The spatial structure is represented by a 2D lattice with periodic boundary conditions. Here, N agents are distributed randomly across the cells, and each cell contains at most one agent. Each cell maintains a resource level that varies both spatially and temporally. We define a Source of Resources (SoR) as a focal point that generates spatial resource gradients in the environment, and these SoRs serve as simplified representations of the natural foraging areas commonly found near rivers, lakes, and coastlines. Each SoR creates a gradient where resource availability typically decreases with increasing distance from the SoR. In addition, multiple SoRs may coexist, thereby forming overlapping zones of resource abundance.

In this model, each agent accumulates resources (represented by the agent's fitness value) through interactions, and local prosperity is defined by a resource threshold $\theta_{x,y}$ for each cell (x,y) , where $0 \leq \theta_{x,y} \leq 1$. Agents with fitness values that are less than the threshold $\theta_{x,y}$ are more likely to migrate and update their strategies, and agents with fitness values greater than the threshold remain unchanged. Therefore, locations with lower thresholds impose less pressure for behavioral change, indicating that these locations are prosperous and rich in resources. Here, the threshold $\theta_{x,y}$ is determined by the cumulative influence of all SoRs and is calculated as follows:

$$\theta_{x,y} = \frac{D_{x,y} - D_{\min}}{D_{\max} - D_{\min}}, \quad D_{x,y} = \sum_{i=1}^{n_{SoR}} d_{x,y}^{(i)} \quad (4.1)$$

where n_{SoR} denotes the number of SoRs, $d_{x,y}^{(i)}$ denotes the Euclidean distance from cell (x,y) to the i -th SoR, calculated under periodic boundary conditions, and D_{\min} and D_{\max} denote the minimum and maximum values of $D_{x,y}$ across the entire grid, respectively.

We examine two spatial configurations, which we refer to as 1-SoR and 2-SoR. In the 1-SoR configuration (a 200×200 grid), a single SoR generates a concentric resource gradient, capturing the essential geographical pattern of an oasis-like environment (Figure 4.1a). In the 2-SoR configuration (a 400×200 grid), two SoRs generate a corridor of resource gradient, capturing the essential geographical pattern of riverine or coastal environments where resources are distributed along a line (Figure 4.1b).

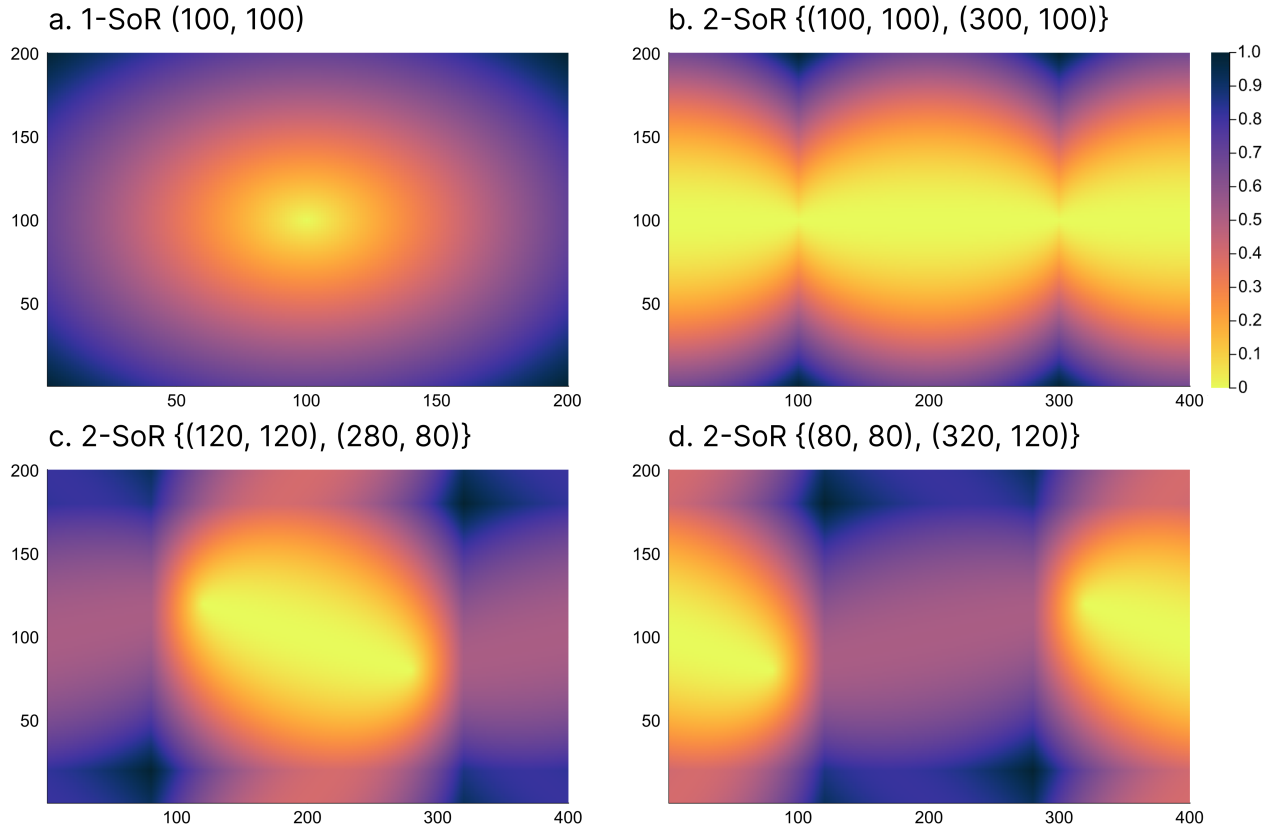


Figure 4.1: Spatially heterogeneous prosperity patterns generated by SoR(s). The colors indicate the resource threshold $\theta_{x,y}$. (a) A single SoR located at $(100, 100)$ on a 200×200 grid generates a concentric resource gradient. (b) Two SoRs located at $(100, 100)$ and $(300, 100)$ on a 400×200 grid generate a band-shaped resource gradient. (c) and (d) Examples of the stochastic movement of SoRs that dynamically reshapes the resource landscapes.

EV is modeled through the stochastic movement of SoRs, reflecting the unpredictable nature of the landscape dynamics observed during the MSA in Africa. Each SoR moves to a randomly selected adjacent cell within the Moore neighborhood with a probability p_{EV} ($0 \leq p_{EV} \leq 1$) at each time step, and the direction is selected uniformly at random from the eight neighboring cells. In this process, the parameter p_{EV} governs the intensity of the EV, where $p_{EV} = 0$ corresponds to a static environment, and higher p_{EV} values represent more intense EV.

Throughout this chapter, the neighborhood is defined as the Moore neighborhood (i.e., eight neighboring cells). This choice better approximates the continuous spatial movement of SoRs and mobile agents than the von Neumann neighborhood (i.e., four orthogonal cells),

where movement is restricted to only cardinal directions. In addition, for distance calculations, particularly when determining resource gradients from SoRs, the Euclidean distance is employed to produce smooth, circular gradients that better represent natural resource distributions than other metrics, e.g., the Manhattan or Chebyshev distances.

Game

Games represent cooperative or competitive interactions between agents that involve the gain or loss of resources. Each agent holds a strategy, either cooperation (C) or defection (D), which determines its behavior in interactions. In every time step, each agent plays pairwise games with all its neighbors and accumulates a payoff π_j , which is then converted into fitness ω_j ($j \in [1, \dots, N]$, $0 < \omega_j < 1$), representing the agent's resource level.

The payoff matrix of the game is defined as follows:

$$\begin{array}{c|cc} & C & D \\ \hline C & R & S \\ D & T & P \end{array} \quad (4.2)$$

where $R = 1$, $0 < T < 2$, $-1 < S < 1$, and $P = 0$. To ensure the robustness of the results across a range of social dilemma contexts, we consider various game structures, including the Prisoner's Dilemma ($T > R > P > S$), Stag Hunt ($R > T > P > S$), and Snowdrift ($T > R > S > P$) games.

The accumulated payoff π_j is transformed into the fitness ω_j using a sigmoid function as follows:

$$\omega_j = \frac{1}{1 + \exp(-k(\pi_j - \pi_0))} \quad (4.3)$$

where k determines the steepness of the sigmoid curve, and π_0 sets the baseline payoff at which $\omega_j = 0.5$. Here, we set $k = 1$ for moderate sensitivity and set $\pi_0 = 4.0$ to center the sigmoid around common payoff values found in mixed-strategy populations. Given that each agent can accumulate payoffs from up to eight of its neighbors, the theoretical payoff range is $8S$ to $8R$ and $8P$ to $8T$ for cooperators and defectors, respectively. With our parameter constraints, this yields a payoff range of $-8 < \pi_j < 16$.

Migration

At each time step, agents migrate if their fitness ω_j is less than the resource threshold $\theta_{x,y}$ at their current location. Any agent that meets this condition migrates with probability p_M and remains at the location with the complementary probability $1 - p_M$. The migration direction follows a resource-oriented bias, where an agent moves toward a neighboring cell with the lowest $\theta_{x,y}$ value with probability p_{SoR} (SoR orientation) and moves randomly within the neighborhood

with the complementary probability $1 - p_{SoR}$. Cells occupied by other agents are excluded from the candidate destinations. The agents migrate asynchronously in a randomized order to avoid movement conflicts.

Strategy update

At each time step, agents update their strategies synchronously if their fitness ω_j is less than the resource threshold $\theta_{x,y}$. Any agent that meets this condition adopts the strategy of the most successful neighbor (i.e., the neighbor with the highest fitness). This process is subject to mutation, where the adopted strategy is replaced by the opposite strategy (e.g., from C to D or vice versa) with probability μ .

We note that asynchronous updating [90, 91] is more realistic and the choice of updating protocol can significantly affect outcomes in densely packed models [90]. However, unlike densely connected lattice models where agents interact with many neighbors simultaneously, our agents typically interact with only a few neighbors on each resource patch. This sparsity reduces the interdependence between neighboring strategy updates, making the dynamics largely insensitive to the updating protocol.

Evaluation

To investigate the effects of EV and agent mobility on the evolution of cooperation, simulations are performed under a range of parameter configurations, as shown in Table 4.1.

Each configuration is evaluated through 100 independent trials of 10000 generations each. As the primary outcome measure, we compute the cooperation rate ϕ_C , which is defined as the average proportion of agents employing the C strategy at the end of each generation (following the strategy update process), averaged over both the final 5000 generations and all 100 independent trials.

4.2 Results

Influence of environmental variability and agent mobility

Figure 4.2 shows the combined effects of EV (p_{EV}) and agent mobility (p_M) on the cooperation rate ϕ_C . As can be seen, in stable environments ($p_{EV} = 0$) or with low agent mobility ($p_M \lesssim 0.2$), cooperation fails to evolve. In contrast, with sufficient agent mobility ($p_M \gtrsim 0.2$), even modest EV ($p_{EV} = 0.1$) promotes cooperation; however, further variability ($p_{EV} > 0.1$) does not enhance cooperation. In addition, agent mobility promotes cooperation with any level of EV ($p_{EV} > 0$).

Table 4.1: Model parameters used in the simulations.

Parameter	Description	Value options
$W \times H$	Grid dimensions	$200 \times 200, 400 \times 200$
N	Number of agents	$\{500, 1000, 2000, 4000, 8000, 16000\}$
ϕ_C^0	Initial frequency of cooperators	$\{0, 0.5, 1\}$
n_{SoR}	Total number of SoRs	$\{1, 2\}$
p_{EV}	Probability of SoR shift; controlling the intensity of EV	$\{0, 0.1, \dots, 1\}$
R	Payoff for mutual cooperation	1
T	Payoff for defection against cooperator	$\{0, 0.1, \dots, 2\}$
P	Payoff for mutual defection	0
S	Payoff for cooperation against defector	$\{-1, -0.9, \dots, 1\}$
p_M	Probability of migration for agents below threshold	$\{0, 0.1, \dots, 1\}$
p_{SoR}	Probability of migrating toward SoR	$\{0, 0.1, \dots, 1\}$
μ	Mutation probability in strategy update	$\{0, 0.01\}$

For a comparison with the other models, refer to Table A.1 in the Appendix.

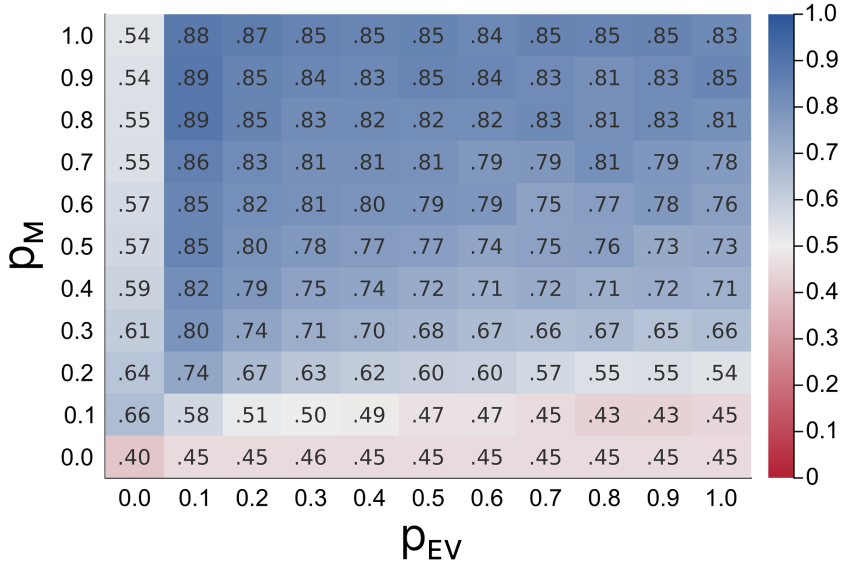


Figure 4.2: Influence of EV (p_{EV}) and agent mobility (p_M) on the cooperation rate (ϕ_C). The figure shows that cooperation emerges only when both $p_{EV} \gtrsim 0.1$ and $p_M \gtrsim 0.2$, with neither factor alone being sufficient to promote cooperation. Each cell shows the mean value over 100 independent runs. The results are shown for a representative parameter set ($N = 1000$, $\phi_C^0 = 0.0$, 2-SoR, $T = 1.2$, $S = -0.2$, $p_{SoR} = 0.1$, $\mu = 0.01$). Qualitatively similar patterns are observed for other parameter configurations. The standard deviations across runs are less than 0.15 for all cells.

Figure 4.3 shows the role of EV in the evolution of cooperation. This representative simulation is presented to understand the temporal dynamics underlying the statistical patterns

displayed in Figure 4.2. Whereas Figure 4.2 considers fixed variability levels throughout the simulation, here we apply a cyclic p_{EV} alternating between stable and variable conditions every 2000 generations over a total of 10000 generations. Under these cyclic conditions, cooperation initially increases to slightly less than 50% during the first stable phase and then plateaus, as shown in Figure 4.3a. A pronounced increase is observed once the system enters the variable phase, which reinforces the conclusion that EV plays a pivotal role in promoting cooperation.

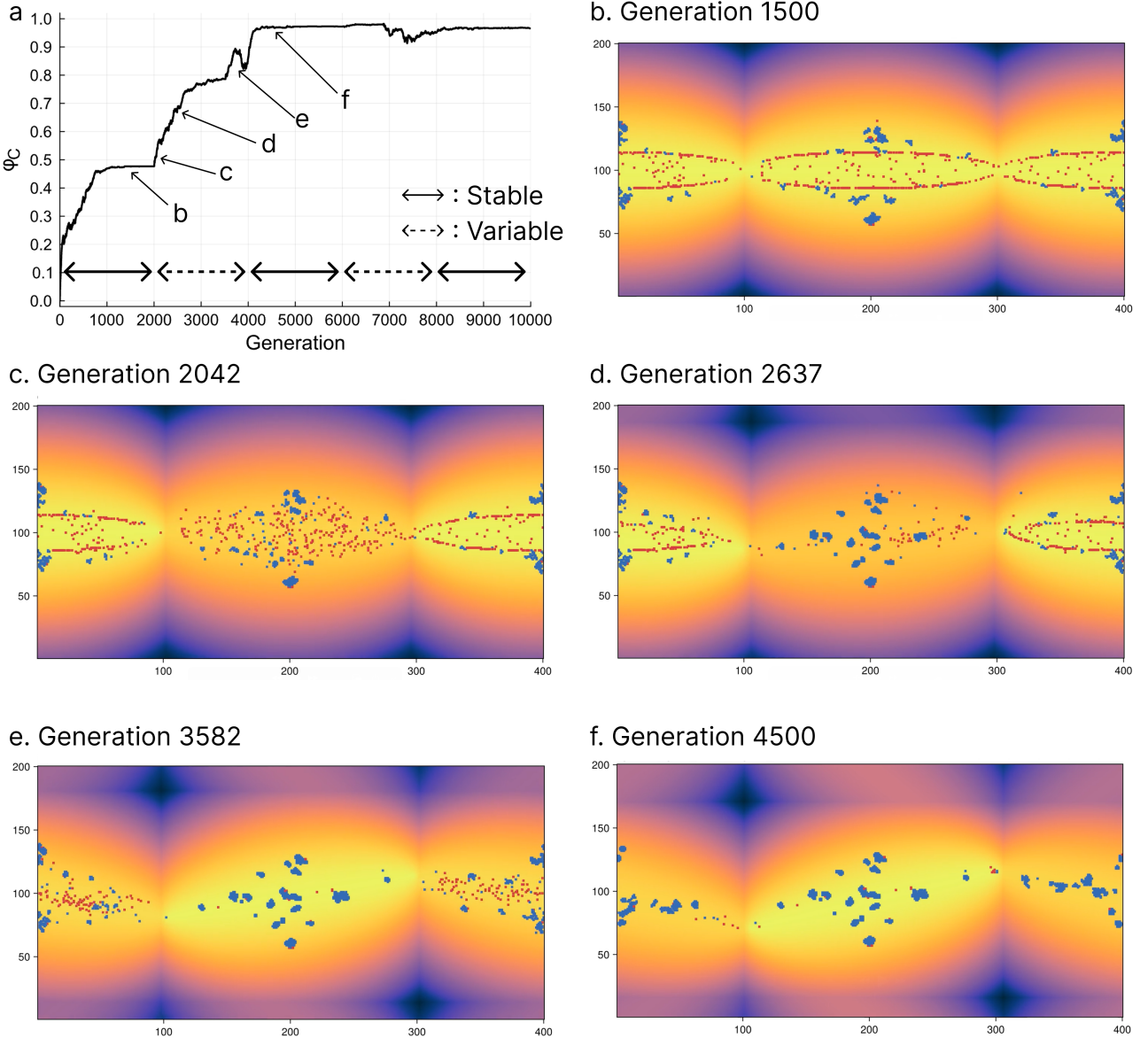


Figure 4.3: Temporal dynamics under cyclic EV. The figure demonstrates that EV drives cooperation by disrupting stable defector groups in resource-rich areas and facilitating the formation of multiple small cooperator groups. (a) Cooperation rate over 10000 generations with p_{EV} alternating between stable ($p_{EV} = 0$) and variable ($p_{EV} = 0.1$) phases every 2000 generations. (b)–(f) Spatial snapshots at each generation. Blue and red dots represent cooperators and defectors, respectively. Background colors indicate the resource threshold $\theta_{x,y}$ as in Figure 4.1. Parameter settings: $N = 1000$, $\phi_C^0 = 0.0$, 2-SoR, $T = 1.2$, $S = -0.2$, $p_M = 1.0$, $p_{SoR} = 0.1$, $\mu = 0.01$.

The observed dynamics can be understood as a three-stage process: (i) the formation of a few large defector groups fixed in resource-rich areas, (ii) their collapse induced by EV, and (iii) subsequent emergence of several small cooperator groups. Figures 4.3b–f show snapshots from the simulation presented in Figure 4.3a. A full video showing this process is provided in the [Appendix](#). In the first stable phase as shown in Figure 4.3b, the agents in prosperous areas have no need to cooperate or move, whereas those in less prosperous areas must cooperate or move to prosperous areas. At the boundaries between these two areas, fixed walls are formed by defectors who do not need to change their strategies or move further. During the next variable phase as shown in Figures 4.3c–e, agents located on boundaries are forced to cooperate or move due to the environmental changes, thereby leading to the collapse of the stable defector group as shown in the central area of Figure 4.3c. In place of the defector group, the agents form several small cooperator groups to survive even in severe environmental conditions (Figure 4.3d). Then, the same process occurs in the areas at both ends of the figure (Figures 4.3e and f).

In contrast, cooperation cannot evolve if the agent mobility is insufficient relative to the intensity of the EV (refer to the lower area of Figure 4.2), which occurs because excessively rapid SoR movement prevents the formation of both defector structures and small cooperator groups, as shown in Figure 4.4. Thus, EV and sufficient agent mobility promote cooperation by preventing fixed defector structures and encouraging the agents to form cooperator groups for survival.

Influence of other parameters on cooperation rate

To gain further insights into the findings presented above and assess their robustness, we investigated the effects of additional parameters, including the population size (N), the number of SoRs (n_{SoR}), the initial frequency of cooperators (ϕ_C^0), the SoR orientation (p_{SoR}), the payoff parameters (T, S), and the mutation rate (μ).

Population size

Larger population size promotes cooperation to some extent, as shown in Figure 4.5, because the cooperators can more easily find other cooperators when the population size is sufficiently large.

Another notable observation is that the cooperation rates for $(p_{EV}, p_M) = (0.0, 0.1)$ (red dashed line) and $(0.1, 0.1)$ (blue dashed line) exhibit a crossover at approximately $N = 2000$. For small populations ($N < 2000$) with low agent mobility, cooperation evolves more readily without EV. In stable environments ($(p_{EV}, p_M) = (0.0, 0.1)$), both the defector and cooperator groups persist once established, although the formation of these groups is slow due to the low agent mobility. In contrast, EV with low agent mobility ($(p_{EV}, p_M) = (0.1, 0.1)$) creates perpetual fluidity that prevents the formation of both structures.

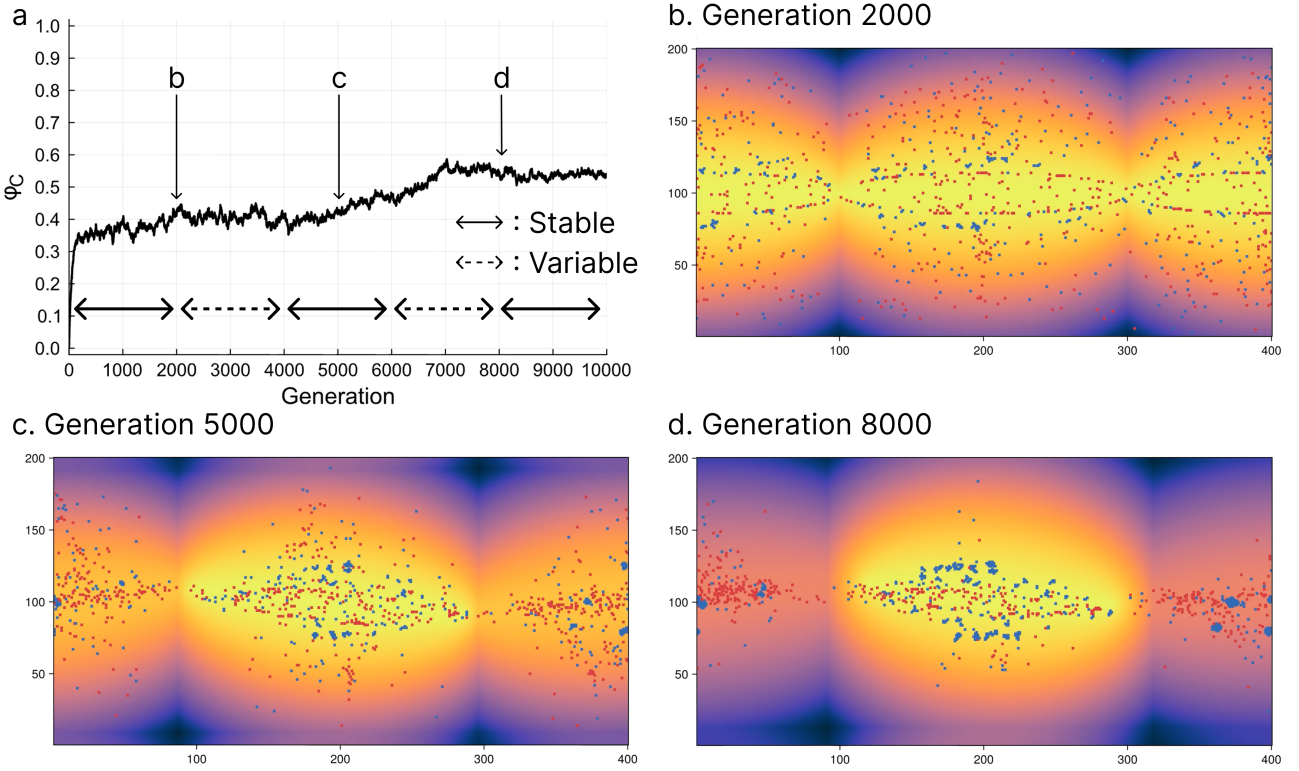


Figure 4.4: Temporal dynamics under cyclic EV with low agent mobility. In contrast to Figure 4.3 ($p_M = 1.0$), here lower mobility ($p_M = 0.1$) prevents agents from keeping up with the EV. As a result, cooperation fails to evolve. All other parameters and the interpretation of the visual elements are the same as in Figure 4.3.

Larger populations alter this relationship. Larger populations increase the encounter rate among cooperators, which allows for the formation of cooperator groups even under EV. In stable environments, the structures remain fixed, thereby limiting the impact of the higher encounter rate. In contrast, the higher encounter rate in fluid environments facilitates group formation. Thus, EV becomes advantageous for cooperation above the critical population size.

A less prominent but similar crossover occurs at approximately $N = 8000$ between $(p_{EV}, p_M) = (0.0, 0.1)$ (red dashed line) and $(p_{EV}, p_M) = (0.0, 1.0)$ (red solid line). This crossover reflects the spatial constraints of the defector groups in stable environments ($p_{EV} = 0$). For $N \lesssim 8000$, high mobility ($p_M = 1.0$) allows more agents to reach the resource-rich areas where cooperation is not required. In contrast, low mobility ($p_M = 0.1$) keeps the agents in peripheral areas where cooperation is required for survival.

However, larger populations ($N \gtrsim 8000$) exhibit three nested zones: central rich areas, where cooperation is not required; surrounding moderate areas, where the agents can survive through cooperation; and the most peripheral harsh areas, where agents cannot survive even with cooperation because the resource threshold exceeds what can be provided through cooperation. Under these conditions, high mobility allows the agents to escape from the harsh areas to the moderate cooperative areas, whereas low mobility traps the agents in the harsh areas. In addition, the central rich areas have already reached their physical capacity due to the large

population; thus, further population increases have no effect in these areas. Consequently, the effect of mobility on the cooperation rate (ϕ_C) reverses as the population size increases.

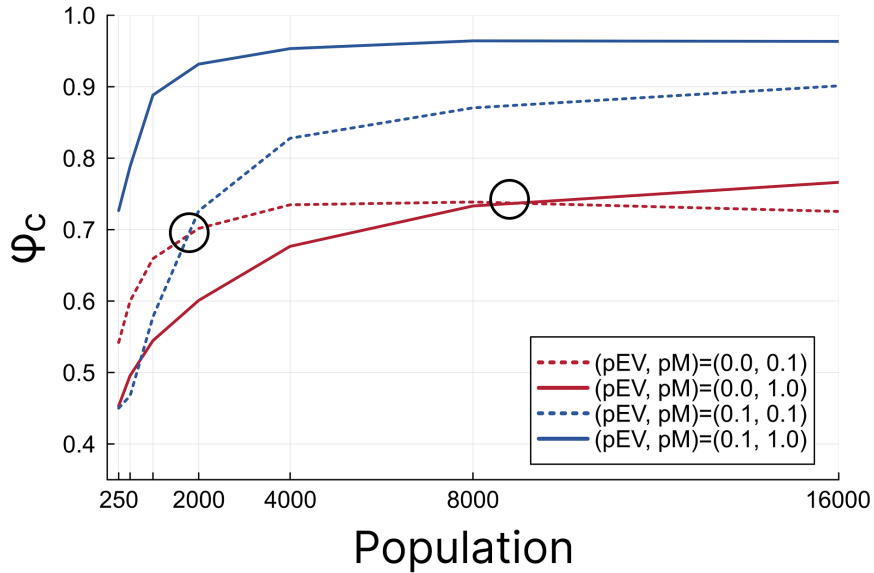


Figure 4.5: Influence of population size (N) on cooperation rate (ϕ_C). The figure shows two crossovers: at $N \approx 2000$ between $(p_{EV}, p_M) = (0.0, 0.1)$ (red dashed) and $(0.1, 0.1)$ (blue dashed), and at $N \approx 8000$ between $(0.0, 0.1)$ (red dashed) and $(0.0, 1.0)$ (red solid). These crossovers reflect how population size alters the relative benefits of EV and mobility through changes in cooperator encounter rates and spatial resource distribution. Parameter settings: $\phi_C^0 = 0.0$, 2-SoR, $T = 1.2$, $S = -0.2$, $p_{SoR} = 0.1$, $\mu = 0.01$. The results for $N = 32000$ are omitted because they exhibited negligible differences from $N = 16000$.

Number of SoRs and initial cooperation rate

Both the number of SoRs (n_{SoR}) and the initial frequency of cooperators (ϕ_C^0) have a significant influence on the results. While the 2-SoR configuration forms large band-shaped defector groups (Figure 4.3b), the 1-SoR configuration only forms a small, circular resource-rich area (Figure 4.6b). When a large defector group collapses and is replaced by small cooperator groups, as observed with the 2-SoR setting, the impact on the overall system is substantial. In contrast, under the 1-SoR setting, when a small defector group undergoes the same replacement, the effect is less conspicuous than in the 2-SoR setting (Figure 4.6a). In terms of ϕ_C^0 , initiation with no cooperators ($\phi_C^0 = 0$) in the 2-SoR configuration results in large defector groups, whereas intermediate or full cooperation ($\phi_C^0 = 0.5$ or 1) maintains the large structure but with a higher cooperator frequency within it (Figure 4.7). Consequently, these conditions mask the significant effects of defector group collapse and cooperator group formation observed in Subsection 4.2.

We also confirmed that changing the distance metric from Euclidean to the Chebyshev or Manhattan distance alters the size and shape of the groups, thereby affecting the results. How-

ever, these effects are primarily attributed to differences in the group size rather than the shape. Thus, comparisons among these distance metrics can be interpreted as theoretically equivalent to the comparison between the 1-SoR and 2-SoR settings. Essentially, the formation of large defector groups in stable environments is the critical prerequisite for the results described in Subsection 4.2.

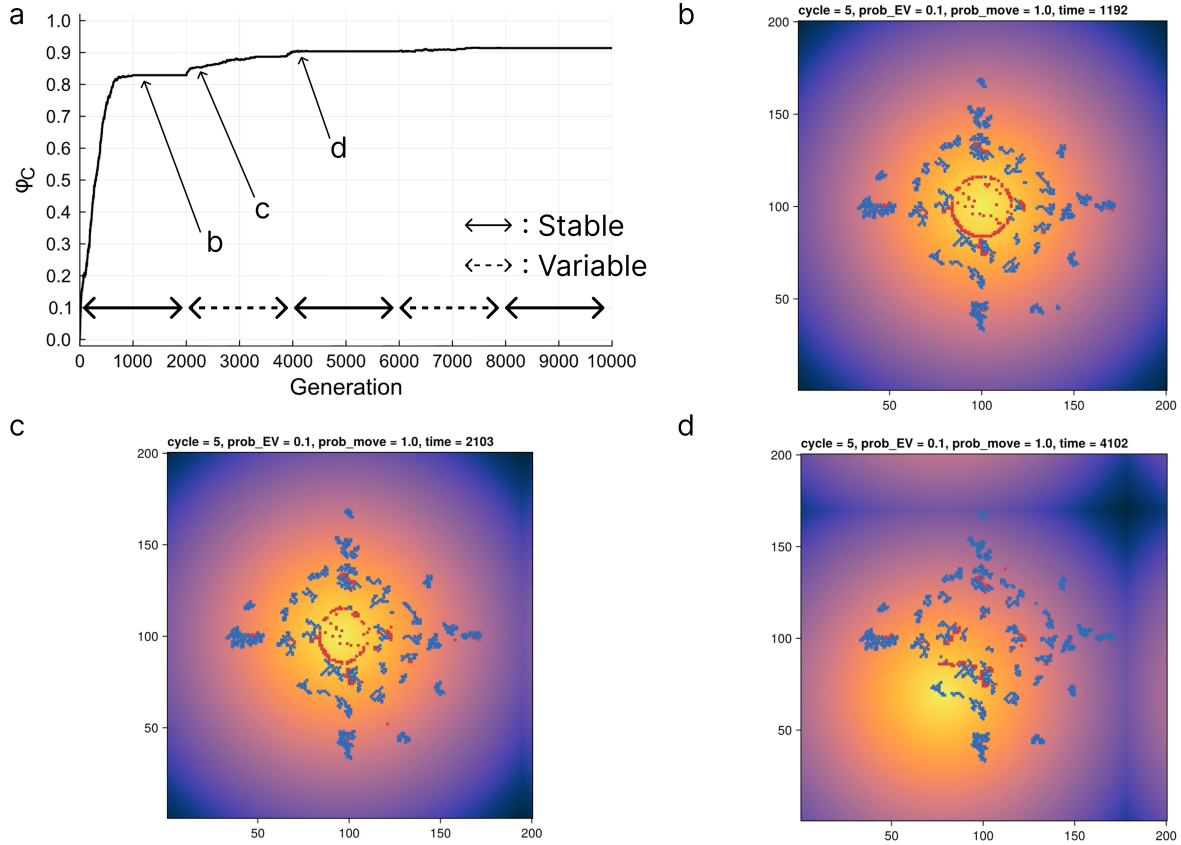


Figure 4.6: Temporal dynamics under cyclic EV in the 1-SoR configuration. The figure shows that the 1-SoR configuration forms only a small circular resource-rich area, resulting in a less pronounced impact of defector group collapse on overall cooperation levels compared to Figure 4.3 (2-SoR). All other parameters and the interpretation of the visual elements are the same as in Figure 4.3.

SoR orientation

SoR orientation (p_{SoR}) noticeably influences the cooperation rate (Figure 4.8). Increasing p_{SoR} from 0 to 0.1 improves cooperation rates by approximately 20%–40% if $p_{EV} > 0$. However, further increases in p_{SoR} beyond 0.2 reduce the cooperation rate. This reduction occurs because excessive p_{SoR} increases the likelihood of agent collisions, which in turn hinders effective migration. These findings suggest that some randomness in the agent mobility is required to maintain a high level of cooperation.

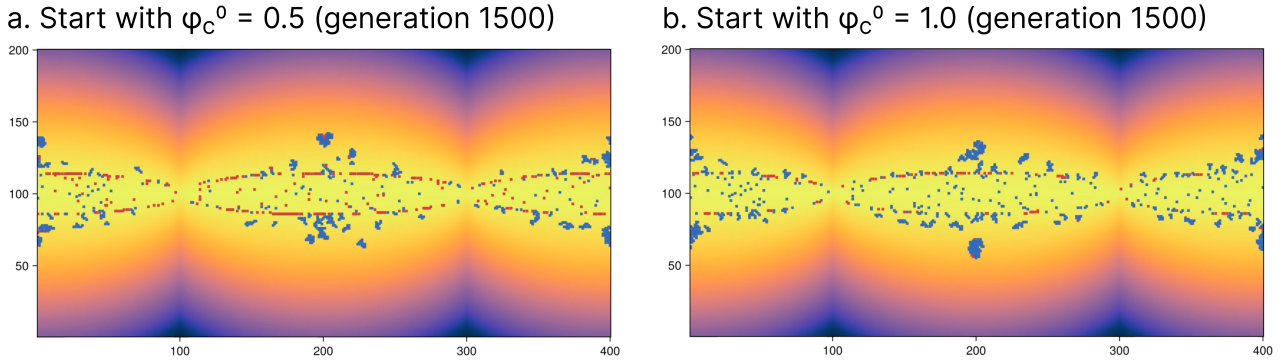


Figure 4.7: Central resource-rich areas under $\phi_C^0 = 0.5$ or 1.0 . The figure shows that higher initial cooperation rates maintain larger cooperative structures in resource-rich areas, masking the effects of defector group collapse and cooperator group formation observed with $\phi_C^0 = 0.0$. All parameters (except ϕ_C^0) and the interpretation of the visual elements are the same as in Figure 4.3.

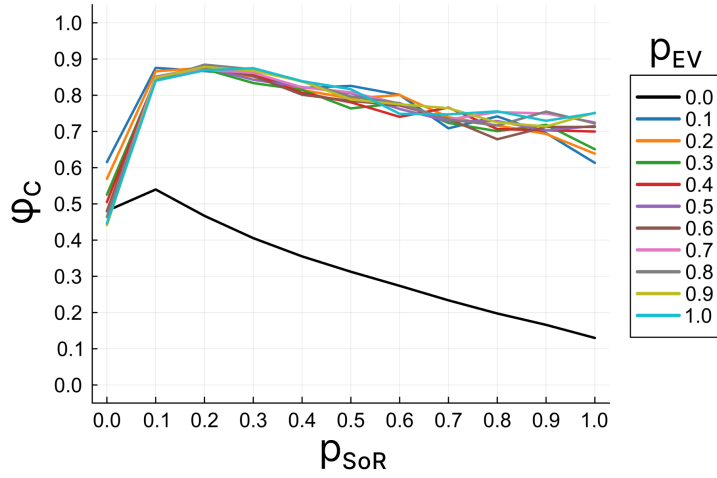


Figure 4.8: Influence of SoR orientation (p_{SoR}) on the cooperation rate (ϕ_C). The figure shows that moderate SoR orientation ($p_{SoR} \approx 0.1$) maximally promotes cooperation, while excessive p_{SoR} reduces cooperation due to increased agent collisions that hinder effective migration. Parameter settings: $N = 1000$, $\phi_C^0 = 0.0$, 2-SoR, $p_M = 1.0$, $T = 1.2$, $S = -0.2$, $\mu = 0.01$.

Payoff parameters and mutation rate

We also investigated the effects of varying the values of the payoff parameters (T, S) across several game structures and the mutation rate μ (including $\mu = 0$ and $\mu = 0.01$). While these variations did not yield qualitatively new insights, they confirmed the robustness of the observed patterns. For completeness, the corresponding results are provided in the [Appendix](#).

4.3 Summary

While the 2-level model in Chapter 3 is a natural extension of the base model, its unique structure limits direct comparison with previous studies on cooperation and migration. To

address this limitation, this chapter adopts a standard 2D lattice space without explicit group structures, a framework widely used in the literature. The model incorporates unpredictable EV by implementing SoRs that move randomly across the 2D space, generating dynamic spatial heterogeneity in resource availability. Agents accumulate resources through cooperative or competitive interactions, and the agents with lower resource levels are more likely to migrate to neighboring cells and update their strategies.

The results demonstrate the following key findings: (i) with sufficient agent mobility, even modest levels of EV promote cooperation; however, further variability does not enhance cooperation; (ii) agent mobility promotes cooperation in the presence of EV; (iii) these effects occur because EV disrupts a small number of large stable defector groups that form in resource-rich areas, and agent mobility enables the formation of numerous small cooperator groups at those sites. These findings demonstrate that EV and agent mobility jointly promote cooperation by preventing fixed defector structures and encouraging the formation of cooperator groups for survival.

The next chapter, Chapter 5, synthesizes and compares the findings from all three models to identify common mechanisms and discuss the broader implications and limitations for understanding the evolution of cooperation under EV.

Chapter 5

Conclusion

This dissertation has investigated whether and how EV promotes the evolution of cooperation using three distinct models presented in Chapters 2 through 4. This chapter synthesizes the results across the models to answer the central research question. Subsequently, we discuss the broader theoretical implications and significance. Finally, we acknowledge the limitations of the study and outline potential directions for future research.

5.1 Summary and cross-model comparison

This section synthesizes the results and mechanisms from the three models presented in this dissertation, highlighting their commonalities and distinctions. The central research question underlying this dissertation is whether and how EV facilitates the evolution of cooperation. Chapter 2 examined the effects of EV on cooperation in the absence of migration. Although migration is a significant factor in the Middle Stone Age (MSA) context, it was excluded in the chapter to isolate the direct impact of EV. Building on this, Chapter 3 investigated the joint effects of EV and migration on cooperation by introducing migration into the group-structured model. Finally, Chapter 4 transitioned to a 2-dimensional spatial framework, a widely established structure in the literature. Table 5.1 provides an overview of the structural features and key findings of the three models.

Beyond this phenomenological comparison, a deeper synthesis is required to uncover the fundamental dynamics governing the evolution of cooperation under EV. Given that the three models employ distinct spatial structures and interaction rules, the consistent positive effect of EV implies the existence of a robust, model-independent principle. Conversely, the divergent outcomes regarding migration suggest that its impact is heavily mediated by structural constraints. To disentangle these factors, the following subsections address three critical questions: (i) why EV promotes cooperation across the three structurally different models; (ii) why the impact of migration differs between the 2-level model and the 2D model; and (iii) how the 2D model relates to the previous literature on cooperation and migration.

Table 5.1: Cross-model comparison of the key features and findings

Chapter	Model overview	Effects of EV and migration
2 The base model	1-level model (group agents only); agents on a 1D circular structure; no migration; dynamic interaction network via rewiring; EV types: RV (regional variability by shifting SoR), UV (universal variability by fluctuating threshold), and CV (combined variability of RV and UV).	(1) RV promotes cooperation. (2) UV has weak effect. (3) CV reflects additive effects of RV and UV.
3 The 2-level model with migration	2-level model (group and individual agents); groups on a 1D circular structure; individuals migrate between neighboring groups; dynamic interaction networks (weight updating) at both levels; EV by shifting SoR.	(1) EV promotes cooperation at both levels. (2) Migration has negligible effect on group-level cooperation. (3) Moderate migration promotes individual-level cooperation, whereas excessive migration hinders it.
4 The 2-dimensional model with migration	1-level model (individual agents only); agents on a 2D lattice; interact with neighbors; migration based on local resource thresholds; EV by shifting SoRs.	(1) EV promotes cooperation when mobility is sufficient. (2) Migration promotes cooperation in the presence of EV.

(i) Why does EV promote cooperation?

Despite the structural differences among the three models, a consistent pattern emerged: EV promotes the evolution of cooperation. The common mechanism is summarized as follows:

1. In static environments, defectors (D_s) exploit cooperators (C_s) and establish dominant structures.
2. EV disrupts this stable dominance, generating stochastic opportunities for not only D_s but also C_s to become resource-rich.
3. Network effects—driven by relationship updating or spatial clustering—selectively maintain the dominance of C_s that emerges stochastically, whereas the dominance of D_s is not maintained.

This mechanism applies to each model as follows. In the lists below, the numbered steps correspond directly to the three stages outlined above.

- Chapter 2 The base model:

1. In static environments, D_s establish dominance.

2. Regional Variability (RV) fluctuates the strategy distribution, creating opportunities also for *Cs*.
3. The link rewiring mechanism maintains the dominance of *Cs* that emerges by chance, whereas the dominance of *Ds* is not maintained.

On the other hand, Universal Variability (UV) does not generate sufficient fluctuations in strategy distribution, and thus does not create chance opportunities for *Cs*.

- Chapter 3 [The 2-level model with migration](#) at the group level:
 1. In static environments, *Ds* establish dominance.
 2. EV fluctuates the group-level resources and strategy distribution, creating opportunities also for *Cs*.
 3. The relationship weight updating mechanism strengthens the cooperative relationships, but not the uncooperative ones.
- Chapter 3 [The 2-level model with migration](#) at the individual level:
 1. In static environments with migration, per-capita resources are equally and statically distributed, leading to *D* dominance.
 2. EV generates resource-rich individuals (*Cs* and *Ds*), allowing them to remain in their group without migration or strategy updates.
 3. When individuals remain in a group, the relationship weight updating mechanism strengthens cooperative relationships, but not uncooperative ones.
- Chapter 4 [The 2-dimensional model with migration](#):
 1. In static environments with migration, *Ds* form large stable clusters.
 2. EV disrupts these stable *D* clusters, forcing them to migrate or update their strategies.
 3. The network effect corresponds to spatial clustering; mobile *Cs* form clusters and gain benefits through mutual cooperation, whereas *Ds* derive no reciprocal advantages from forming their own clusters. Consequently, *C* clusters are self-reinforcing, whereas *D* clusters are not.

This consistent applicability suggests that the evolution of cooperation under EV is not a model-specific artifact but a fundamental phenomenon. In essence, EV functions as a catalyst that disrupts the static entrenchment of defectors, thereby allowing network mechanisms to selectively retain the cooperative structures that emerge during these stochastic fluctuations. This implies that environmental dynamics are as critical as network dynamics in unlocking the evolution of cooperation.

(ii) Why does the impact of migration differ between the 2-level model and the 2D model?

While EV promotes cooperation consistently, the effect of migration varies between the 2-level model (Chapter 3) and the 2D model (Chapter 4). In the 2-level model, excessive migration hinders cooperation, whereas in the 2D model, migration consistently promotes it under EV. This discrepancy arises from the fundamental difference in the time required to establish cooperative relationships in each model.

In the 2-level model, the formation of cooperative networks relies on the gradual accumulation of interaction weights. This process requires time. Excessive migration disrupts this accumulation, as individuals leave their groups before stable cooperative relationships can mature. Therefore, individuals must remain in the same group for a sufficient duration to foster the strong ties necessary for cooperation.

In contrast, in the 2D model, cooperative relationships are determined solely by spatial adjacency and are established instantaneously. When cooperators migrate and settle next to each other, they immediately form a functional cooperative relationship without the need for a time-consuming weight-building process. Thus, migration does not reset the progress of relationship formation but simply rearranges the configuration.

This comparison suggests a general insight: excessive mobility hinders cooperation when the formation of relationships requires time or relies on a history of interaction.

(iii) How does the 2D model relate to the previous literature on cooperation and migration?

The relationship between migration and cooperation has been a subject of debate in evolutionary game theory. Classical literature generally posits that mobility hinders cooperation. Dugatkin and Wilson (1991) [77] showed that Rover—a mobile All-D agent—can overtake cooperative strategies (e.g., All-C and Tit-for-Tat (TFT)) if the migration cost is low. Cohen et al. (2001) [92] theoretically demonstrated that stable interaction structure, which they termed “context preservation”, is necessary for the sustainability of cooperative relationships. According to this view, migration is detrimental because it disrupts the stable social context required for cooperation.

In contrast, more recent studies have suggested that mobility can facilitate cooperation under specific conditions. Vainstein et al. (2007) [79], titled “Does mobility decrease cooperation?”, demonstrated that in low-density spatial environments, mobility allows isolated cooperators to find each other, thereby promoting the formation of cooperative clusters. Building on Vainstein’s framework, subsequent studies on various research focuses [83–89] have identified conditions under which migration promotes cooperation.

The 2D model (Chapter 4) also extends Vainstein’s framework, focusing on the influence of

EV. In this model, migration consistently promotes cooperation. This result is consistent with Vainstein's finding that mobility promotes cooperation in low-density spatial environments. However, the 2D model demonstrates complex population structure dynamics that are not observed in Vainstein's model. This is because Vainstein's model does not consider EV and lacks spatial heterogeneity, whereas the 2D model explicitly focuses on the influence of EV.

Regarding the classical literature, the results in the 2D model appear to oppose the view that mobility hinders cooperation. However, this apparent discrepancy arises because the mobility in the 2D model is not random but is triggered by local resource depletion, which does not disrupt the stable formation of cooperative clusters. Therefore, the results in the 2D model do not contradict the classical literature, as they operate under fundamentally different migration mechanisms. Notably, in the 2-level model (Chapter 3), excessive migration hinders cooperation, which is fully consistent with the classical literature.

5.2 Implications and significance

The findings of this dissertation carry implications and significance for the theoretical understanding of cooperation, the variability selection hypothesis (VSH) and related debates in human evolution (the cognitive buffer hypothesis (CBH) and the social brain hypothesis (SBH)), and potential applications to broader contexts.

This dissertation advances the theoretical understanding of cooperation by establishing EV as a robust driver of cooperative behavior. While previous research has examined mechanisms under static conditions, the role of environmental dynamics has remained understudied. The consistent finding across three structurally distinct models suggests that environmental factors deserve greater attention in theoretical frameworks of cooperation. The common mechanism identified in Section 5.1 reveals a fundamental interplay between environmental dynamics and network dynamics, suggesting that cooperation cannot be fully understood by examining social interactions in isolation from environmental context. This perspective integrates with, rather than replaces, established cooperation mechanisms. Specifically, EV does not introduce an entirely new mechanism but rather modulates the effectiveness of existing mechanisms by altering the environmental conditions under which they operate.

The VSH [27, 28] posits that intensified environmental fluctuations during the MSA in Africa favored specialists capable of rapid adaptation. While this hypothesis has been supported by temporal correlations between environmental changes and the emergence of modern human behavior, the causal mechanisms linking EV to specific behavioral traits have remained unclear. The findings of this dissertation provide theoretical support for one component of this link by demonstrating plausible mechanisms through which EV could have promoted cooperative behavior.

Furthermore, these findings contribute to the ongoing debate between the CBH [30–32] and

the SBH [29, 37–43]. The CBH proposes that EV selected for enhanced cognitive abilities, providing a theoretical basis for the VSH. The SBH, often presented as an alternative, argues that social complexity was the primary driver of cognitive evolution. The present findings suggest that EV may have promoted cooperative behavior—a core element of the social complexity emphasized by the SBH. If EV drove not only individual cognitive abilities but also cooperative social behavior, the CBH and the SBH may be complementary rather than competing.

While this dissertation is primarily motivated by questions concerning human evolution in the MSA, the findings have broader implications for understanding cooperation in other contexts. The fundamental mechanism whereby EV promotes cooperation by disrupting defector dominance and enabling cooperator clustering may operate across diverse biological and social systems. Although direct application to other domains is not straightforward, the identified mechanisms hold potential for shedding light on ecological systems or contemporary human societies facing increased environmental risks due to climate change and other factors.

5.3 Limitations and future directions

While this dissertation provides theoretical insights into the role of EV in the evolution of cooperation, several limitations should be acknowledged. The limitations can be broadly categorized into three areas: the absence of empirical validation, the simplification of model assumptions, and the complexity of the simulation approach. These limitations, however, point toward productive directions for future research.

Empirical validation

The first limitation concerns the insufficiency of empirical data to directly validate the simulation models and results. This limitation reflects the inherent scarcity of detailed archaeological and paleoenvironmental data from the MSA in Africa. The models can identify qualitative patterns and mechanisms but cannot predict, for example, the specific magnitude of EV required to produce a given level of cooperation, or the timescales over which cooperative behavior would emerge under particular conditions. Nevertheless, this very scarcity underscores the value of computational simulations: where direct observation of evolutionary processes is infeasible and empirical data remain fragmentary, simulations provide a principled approach to exploring plausible mechanisms and generating testable predictions.

Moreover, the theoretical predictions generated here may guide future empirical investigations by directing attention to specific patterns. The same archaeological or paleoenvironmental data may yield different insights depending on whether researchers approach them with hypotheses regarding the relationship between EV and cooperation. For instance, evidence of long-distance resource transport during the MSA has traditionally been interpreted primarily

as an indicator of expanded home ranges or trading capabilities. With the hypothesis that EV promotes cooperation, however, the same evidence might be re-examined for temporal correlations with periods of intensified climate instability, potentially revealing that such cooperative behaviors emerged specifically during environmentally variable periods.

Model simplification

The second limitation concerns the intentional simplifications made to the models. To isolate the fundamental mechanisms through which EV promotes cooperation, we employed several abstractions in each model component: spatial structure, population structure, EV, interaction, migration, and strategy update.

The spatial structure was represented by regular topologies, specifically 1-dimensional cycle graphs and 2-dimensional lattices. These idealized structures are standard in theoretical investigations, as they facilitate the identification of universal evolutionary mechanisms independent of specific geographic idiosyncrasies. Potential avenues for extending this work include the adoption of more complex network architectures [93–95] or the integration of spatially explicit models grounded in paleoenvironmental reconstructions of the MSA in Africa.

The population structure was represented by non-hierarchical structures (homogeneous group- or individual-level agents) or a minimal 2-level hierarchical structure. Although real-world human social structures exhibit complex fractal organizations [57], restricting the model to simple structures represents a standard methodological approach. This reflects the heuristic that greater complexity diminishes interpretability and tractability while increasing arbitrariness, often obscuring essential mechanisms without significantly altering the results. It is not inconceivable, however, that introducing greater demographic realism, such as life history stages or a 3-tiered social architecture consisting of individuals, families, and bands, might add some nuances to the evolutionary dynamics. Furthermore, the current models assume a constant population size; incorporating demographic fluctuations, such as variations in birth and death rates, could significantly impact the long-term stability of cooperation.

Regarding the EV, the stochastic movement of SoRs effectively captures the landscape dynamics and the consequent unpredictability of resource availability, which are characteristic of the MSA in Africa. While this abstraction provides a robust foundation for future research, subsequent models could incorporate greater environmental realism, for example by calibrating the dynamics to paleoclimatic proxy data from relevant MSA sites.

In terms of interaction, the models adopted a fundamental pairwise game framework restricted to binary strategies of unconditional cooperation or defection. Given the active discourse within evolutionary game theory, however, numerous extensions are conceivable. Future research could explore multi-player games, more complex strategic repertoires such as TFT, reputation-based mechanisms, and social norms. Furthermore, interaction structures

and relationship update rules could be refined based on empirical research and laboratory experiments. Additionally, the unit of interaction—whether it occurs between individuals or groups—warrants deeper investigation to determine how different levels of agency affect the results.

The migration process was triggered by resource scarcity and migration probability, assuming zero migration costs. However, human mobility decisions in the real world are influenced by social factors and other environmental factors. Future models could thus incorporate migration costs [96] and more realistic migration dynamics [83–89], for example by accounting for conflict avoidance, mate-seeking, kinship obligations, and predator avoidance. Another critical dimension is the unit of migration; while the models treat migration as an individual decision, real-world mobility often operates at the level of collective social units rather than individual.

Finally, the strategy updating process has been extensively examined within the framework of cultural evolution [97–99]. Within this field, learning mechanisms for strategy updating are primarily categorized into social learning (SL), individual learning (IL), and their interplay. The models in this dissertation adopted payoff-biased imitation where agents copy the most successful strategies observed within their communication range. This is a specific form of SL. Subsequent models could therefore broaden this scope by incorporating other SL mechanisms such as conformity bias, or integrating IL mechanisms such as reinforcement learning. Furthermore, the fundamental unit of agency warrants further scrutiny, specifically regarding whether adaptation could operate effectively at the level of the group or should be strictly restricted to the individual.

While these strategic simplifications were indispensable for isolating the fundamental mechanisms of cooperation, future research should evaluate the robustness of these findings by systematically integrating the social and environmental complexities inherent in human evolutionary history.

Model complexity

While the previous section addressed the limitations of model simplification regarding the empirical realities of the MSA, there exists a converse methodological limitation: the models employed in this dissertation are, in another sense, too complex for rigorous analytical solution. As a constructive approach, our multi-agent simulations allowed for the reproduction of broad qualitative patterns and the identification of a robust mechanism across different model structures. However, the interplay between EV, agent mobility, and dynamic interaction structures involves high-dimensional, non-linear interactions that resist straightforward mathematical formulation.

Because of this complexity, while we have provided a qualitative description of how EV disrupts defector dominance and allows network effects to retain cooperation, we have not yet

formalized these dynamics into a set of closed-form analytical equations. Consequently, we cannot yet provide precise quantitative predictions, such as the exact mathematical threshold for the magnitude of EV or the specific migration probability required to flip a system from defection to cooperation. The current simulation-based approach identifies that a mechanism works, but analytical modeling is needed to define the exact logical boundaries of where and why it fails or succeeds.

Future research should therefore aim to bridge this gap by developing “minimalist” analytical models. It may be possible to isolate the relationship between EV and the evolution of cooperation in its purest form by reducing the model complexity and utilizing standard analytical tools in evolutionary game theory, such as replicator dynamics or Markov chain analysis, and more broadly, the framework of non-equilibrium statistical mechanics [19, 21]. Such models would not replace the simulations presented here but would complement them by providing a more rigorous logical foundation. Combining the constructive insights from multi-agent simulations with the precision of formal mathematical analysis will ultimately lead to a more sophisticated understanding of the mechanisms that drove the evolution of modern human sociality.

5.4 Concluding remarks

By analyzing three distinct models, this dissertation has established EV as a robust driver of the evolution of cooperation. This chapter demonstrated that the seemingly distinct mechanisms detailed in Chapters 2 through 4 are underpinned by a common principle: EV facilitates cooperation by disrupting the static dominance of defectors and allowing network mechanisms to stabilize emerging cooperators. This consistency indicates that the findings are not model-specific artifacts but represent a consistent and robust pattern in the evolution of cooperation.

Inspired by the VSH, which posits that the evolution of human behavior in the MSA was driven by intensified EV, this dissertation demonstrates a theoretical pathway for the development of cooperative sociality. Beyond its implications for human evolution, this work advances the theoretical understanding of the evolution of cooperation by establishing EV as an integral component of social dynamics. Furthermore, the identified mechanisms could potentially offer broader implications for the emergence and persistence of cooperative systems in other biological and contemporary social contexts facing increased environmental risks.

Despite these contributions, this research is not without limitations, particularly regarding empirical validation, model simplification relative to real-world situations, and model complexity for obtaining analytical solutions. These limitations, however, offer promising avenues for future development. Future work could strive to increase the persuasiveness of these models by validating them against accumulating archaeological and paleo-environmental data. Simultaneously, exploring simpler models that allow for analytical solutions is expected to clarify the

underlying mechanisms with greater mathematical precision. Such integrated approaches will further elucidate the complex relationship between environmental dynamics and the evolution of cooperation, and by extension, provide deeper insights into the evolution of sociality. We hope that the groundwork laid by this dissertation will serve as a meaningful starting point for these future intellectual endeavors.

Appendix

Detailed comparison of the three simulation models

Table A.1 summarizes the key specifications and comparative features of the three simulation models analyzed in Chapters 2, 3, and 4. For details on each model, please refer to the respective chapters in the main text.

Supplementary materials

Supplementary materials for each chapter are available at the following repositories:

- **Chapter 2:** <https://github.com/mas178/Inaba2024>

This repository contains the simulation code, datasets, and scripts for generating the figures.

- **Chapter 3:** <https://github.com/mas178/Inaba2026-2Lvl>

This repository contains the simulation code, datasets, scripts for generating the figures, and the detailed results of the sensitivity analyses regarding the effects of SoR orientation (p_{SoR}), the payoff multiplier b , and the mutation rate μ .

- **Chapter 4:** <https://github.com/mas178/Inaba2025-2D>

This repository contains the simulation code, datasets, scripts for generating the figures, supplementary videos, and the comprehensive results of the robustness checks for the payoff parameters (T, S) and the mutation rate μ .

Table A.1: Detailed comparison of the three simulation models

Component	Ch.2 Base Model	Ch.3 2-Level Model	Ch.4 2D Model
Agent	Group agents (N) only	Groups (N_R) and Individuals (N_F)	Individual agents (N) only
Spatial Structure	1D circular structure	1D circular structure	2D lattice with periodic boundary conditions
Interaction Structure	Dynamic network (undirected, unweighted) via rewiring; Initial degree k_0	Dynamic weights $w_{i,j}$ (init: w_0) on a complete network	Spatial adjacency (Moore neighborhood)
Environmental Variability (EV)	RV (SoR shift): Shift range σ_R ; UV (Threshold θ fluctuation); AR(1) with autoregressive coefficient (β) and SD of the noise term (σ_θ); CV: RV + UV	Shift of an SoR between groups: 1-step shift probability p_{EV}	Shift of SoR(s) on 2D space (Moore neighborhood): 1-step shift probability p_{EV}
Game	Pairwise PGG; Multiplier b ; Contribution $M_i = \max(r_i - \theta, 0)$	Executed at two levels: Pairwise PGG; Multiplier b ; Contribution $c_i = r_i \times w_{i,j}$	Classic pairwise games based on 2×2 payoff table
Migration	Not incorporated	Scarcity-triggered migration between neighboring groups; Migration probability: $\max(1 - r_i^F/\theta_F, 0) \cdot p_M$; Direction: with probability p_{SoR} toward lowest $\theta_{x,y}$, otherwise random	Scarcity-triggered migration across the Moore neighborhood; Migration probability: p_M if $\omega_j < \theta_{x,y}$; Direction: with probability p_{SoR} toward lowest $\theta_{x,y}$, otherwise random
Strategy Update (Reformation in Ch.2)	Update probability: 1 if $r_i < \theta$, otherwise 0; Imitate a successful agent's strategy with probability p_j^R ; Reconnect with successful agents with probability p_j^R ; Mutation rate: μ	Executed at two levels: Update probability: $\max\left(1 - \frac{r_i}{\theta}, 0\right) \cdot p_{SU}$; Imitate a successful agent's strategy with probability $Q(j i)$; Reset weights of updated agents to w_0 ; Mutation rate: μ	Update probability: 1 if $\omega_j < \theta_{x,y}$, otherwise 0; Imitate the most successful neighbor's strategy; Mutation rate: μ

Bibliography

- [1] C. Darwin. On the origin of species. 1859.
- [2] C. Darwin. The descent of man, and selection in relation to sex. 1871.
- [3] W. Hamilton. The genetical evolution of social behaviour. I. *J. theor. biol.* 7.1 (1964), 1–16. DOI: [10.1016/0022-5193\(64\)90038-4](https://doi.org/10.1016/0022-5193(64)90038-4).
- [4] W. D. Hamilton. The genetical evolution of social behaviour. II. *J. theor. biol.* 7.1 (1964), 17–52. DOI: [10.1016/0022-5193\(64\)90039-6](https://doi.org/10.1016/0022-5193(64)90039-6).
- [5] M. A. Nowak, C. E. Tarnita, and E. O. Wilson. The evolution of eusociality. *Nature* 466.7310 (2010), 1057–1062. DOI: [10.1038/nature09205](https://doi.org/10.1038/nature09205).
- [6] P. Abbot, J. Abe, J. Alcock, S. Alizon, J. A. C. Alpedrinha, M. Andersson, et al. Inclusive fitness theory and eusociality. *Nature* 471.7339 (2011), E1–4, author reply E9–10. DOI: [10.1038/nature09831](https://doi.org/10.1038/nature09831).
- [7] M. van Veelen. The general version of hamilton’s rule. *Elife* (2025). DOI: [10.7554/elife.105065.1](https://doi.org/10.7554/elife.105065.1).
- [8] J. M. Smith and G. R. Price. The logic of animal conflict. *Nature* 246.5427 (1973), 15–18. DOI: [10.1038/246015a0](https://doi.org/10.1038/246015a0).
- [9] R. Axelrod and W. D. Hamilton. The evolution of cooperation. *Science* 211.4489 (1981), 1390–1396. DOI: [10.1126/science.7466396](https://doi.org/10.1126/science.7466396).
- [10] M. A. Nowak and K. Sigmund. Evolution of indirect reciprocity by image scoring. *Nature* 393.6685 (1998), 573–577. DOI: [10.1038/31225](https://doi.org/10.1038/31225).
- [11] M. A. Nowak and K. Sigmund. Evolution of indirect reciprocity. *Nature* 437.7063 (2005), 1291–1298. DOI: [10.1038/nature04131](https://doi.org/10.1038/nature04131).
- [12] H. Ohtsuki, C. Hauert, E. Lieberman, and M. A. Nowak. A simple rule for the evolution of cooperation on graphs and social networks. *Nature* 441.7092 (2006), 502–505. DOI: [10.1038/nature04605](https://doi.org/10.1038/nature04605).
- [13] A. Traulsen and M. A. Nowak. Evolution of cooperation by multilevel selection. *Proc. natl. acad. sci. u. s. a.* 103.29 (2006), 10952–10955. DOI: [10.1073/pnas.0602530103](https://doi.org/10.1073/pnas.0602530103).

- [14] M. A. Nowak. Five rules for the evolution of cooperation. *Science* 314.5805 (2006), 1560–1563. DOI: [10.1126/science.1133755](https://doi.org/10.1126/science.1133755).
- [15] S. A. West, A. S. Griffin, and A. Gardner. Evolutionary explanations for cooperation. *Curr. biol.* 17.16 (2007), R661–72. DOI: [10.1016/j.cub.2007.06.004](https://doi.org/10.1016/j.cub.2007.06.004).
- [16] G. Szabó and G. Fáth. Evolutionary games on graphs. *Phys. rep.* 446.4-6 (2007), 97–216. DOI: [10.1016/j.physrep.2007.04.004](https://doi.org/10.1016/j.physrep.2007.04.004).
- [17] M. Perc and A. Szolnoki. Coevolutionary games—a mini review. *Biosystems* 99.2 (2010), 109–25. DOI: [10.1016/j.biosystems.2009.10.003](https://doi.org/10.1016/j.biosystems.2009.10.003).
- [18] M. A. Zaggl. Eleven mechanisms for the evolution of cooperation. *Journal of institutional economics* 10.2 (2014), 197–230. DOI: [10.1017/S1744137413000374](https://doi.org/10.1017/S1744137413000374).
- [19] M. Perc, J. J. Jordan, D. G. Rand, Z. Wang, S. Boccaletti, and A. Szolnoki. Statistical physics of human cooperation. *Phys. rep.* 687 (2017), 1–51. DOI: [10.1016/j.physrep.2017.05.004](https://doi.org/10.1016/j.physrep.2017.05.004).
- [20] S. A. West, G. A. Cooper, M. B. Ghoul, and A. S. Griffin. Ten recent insights for our understanding of cooperation. *Nat. ecol. evol.* 5.4 (2021), 419–30. DOI: [10.1038/s41559-020-01384-x](https://doi.org/10.1038/s41559-020-01384-x).
- [21] M. Jusup, P. Holme, K. Kanazawa, M. Takayasu, I. Romić, Z. Wang, et al. Social physics. *Phys. rep.* 948 (2022), 1–148. DOI: [10.1016/j.physrep.2021.10.005](https://doi.org/10.1016/j.physrep.2021.10.005).
- [22] S. Mcbrearty and A. S. Brooks. The revolution that wasn’t: a new interpretation of the origin of modern human behavior. *J. hum. evol.* 39.5 (2000), 453–563. DOI: [10.1006/jhev.2000.0435](https://doi.org/10.1006/jhev.2000.0435).
- [23] C. S. Henshilwood and C. W. Marean. The origin of modern human behavior: Critique of the models and their test implications. *Curr. anthropol.* 44.5 (2003), 627–651. DOI: [10.1086/377665](https://doi.org/10.1086/377665).
- [24] F. d’Errico, A. Pitarch Martí, C. Shipton, E. Le Vraux, E. Ndiema, S. Goldstein, et al. Trajectories of cultural innovation from the Middle to Later Stone Age in Eastern Africa: Personal ornaments, bone artifacts, and ochre from Panga ya Saidi, Kenya. *J. hum. evol.* 141.102737 (2020), 102737. DOI: [10.1016/j.jhevol.2019.102737](https://doi.org/10.1016/j.jhevol.2019.102737).
- [25] J. Wilkins, B. J. Schoville, R. Pickering, L. Gliganic, B. Collins, K. S. Brown, et al. Innovative Homo sapiens behaviours 105,000 years ago in a wetter Kalahari. *Nature* 592.7853 (2021), 248–252. DOI: [10.1038/s41586-021-03419-0](https://doi.org/10.1038/s41586-021-03419-0).
- [26] A. Bergström, C. Stringer, M. Hajdinjak, E. M. L. Scerri, and P. Skoglund. Origins of modern human ancestry. *Nature* 590 (2021), 229–237. DOI: [10.1038/s41586-021-03244-5](https://doi.org/10.1038/s41586-021-03244-5).

- [27] R. Potts. Evolution and climate variability. *Science* 273.5277 (1996), 922–923. DOI: [10.1126/science.273.5277.922](https://doi.org/10.1126/science.273.5277.922).
- [28] R. Potts. Environmental hypotheses of hominin evolution. *Am. j. phys. anthropol.* 107.S27 (1998), 93–136. DOI: [10.1002/\(sici\)1096-8644\(1998\)107:27+<93::aid-ajpa5>3.0.co;2-x](https://doi.org/10.1002/(sici)1096-8644(1998)107:27+<93::aid-ajpa5>3.0.co;2-x).
- [29] J. T. Faith, A. Du, A. K. Behrensmeyer, B. Davies, D. B. Patterson, J. Rowan, et al. Rethinking the ecological drivers of hominin evolution. *Trends ecol. evol.* 36.9 (2021), 797–807. DOI: [10.1016/j.tree.2021.04.011](https://doi.org/10.1016/j.tree.2021.04.011).
- [30] C. Schuck-Paim, W. J. Alonso, and E. B. Ottoni. Cognition in an ever-changing world: climatic variability is associated with brain size in Neotropical parrots. *Brain behav. evol.* 71.3 (2008), 200–15. DOI: [10.1159/000119710](https://doi.org/10.1159/000119710).
- [31] D. Sol, S. Bacher, S. M. Reader, and L. Lefebvre. Brain size predicts the success of mammal species introduced into novel environments. *Am. nat.* 172.S1 (2008), S63–71. DOI: [10.1086/588304](https://doi.org/10.1086/588304).
- [32] D. Sol. Revisiting the cognitive buffer hypothesis for the evolution of large brains. *Biol. lett.* 5.1 (2009), 130–3. DOI: [10.1098/rsbl.2008.0621](https://doi.org/10.1098/rsbl.2008.0621).
- [33] M. Grove. Speciation, diversity, and Mode 1 technologies: the impact of variability selection. *J. hum. evol.* 61.3 (2011), 306–319. DOI: [10.1016/j.jhevol.2011.04.005](https://doi.org/10.1016/j.jhevol.2011.04.005).
- [34] A. Navarrete, C. P. van Schaik, and K. Isler. Energetics and the evolution of human brain size. *Nature* 480.7375 (2011), 91–93. DOI: [10.1038/nature10629](https://doi.org/10.1038/nature10629).
- [35] M. Will, M. Krapp, J. T. Stock, and A. Manica. Different environmental variables predict body and brain size evolution in Homo. *Nat. commun.* 12.1 (2021), 4116. DOI: [10.1038/s41467-021-24290-7](https://doi.org/10.1038/s41467-021-24290-7).
- [36] J. M. Stibel. Climate change influences brain size in humans. *Brain behav. evol.* 98.2 (2023), 93–106. DOI: [10.1159/000528710](https://doi.org/10.1159/000528710).
- [37] A. Whiten and R. Byrne. The machiavellian intelligence hypotheses. *Machiavellian intelligence: social expertise and the evolution of intellect in monkeys, apes, and humans*. 413 (1988). Ed. by R. W. Byrne, 1–9.
- [38] R. I. M. Dunbar. The social brain hypothesis. *Evolutionary anthropology: issues, news, and reviews: issues, news, and reviews* 6.5 (1998), 178–190. DOI: [10.1002/\(SICI\)1520-6505\(1998\)6:5<178::AID-EVAN5>3.0.CO;2-8](https://doi.org/10.1002/(SICI)1520-6505(1998)6:5<178::AID-EVAN5>3.0.CO;2-8).
- [39] L. Barrett, P. Henzi, and D. Rendall. Social brains, simple minds: does social complexity really require cognitive complexity? *Philos. trans. r. soc. lond. b biol. sci.* 362.1480 (2007), 561–575. DOI: [10.1098/rstb.2006.1995](https://doi.org/10.1098/rstb.2006.1995).

- [40] M. Grove and F. Coward. From individual neurons to social brains. *Camb. archaeol. j.* 18.3 (2008), 387–400. DOI: [10.1017/s0959774308000437](https://doi.org/10.1017/s0959774308000437).
- [41] C. Knight and C. Power. Social conditions for the evolutionary emergence of language. Oxford University Press, 2011. DOI: [10.1093/oxfordhb/9780199541119.013.0037](https://doi.org/10.1093/oxfordhb/9780199541119.013.0037).
- [42] S. C. Hayes and B. T. Sanford. Cooperation came first: evolution and human cognition. *J. exp. anal. behav.* 101.1 (2014), 112–129. DOI: [10.1002/jeab.64](https://doi.org/10.1002/jeab.64).
- [43] R. I. M. Dunbar. The social brain hypothesis - thirty years on. *Ann. hum. biol.* 51.1 (2024), 2359920. DOI: [10.1080/03014460.2024.2359920](https://doi.org/10.1080/03014460.2024.2359920).
- [44] A. R. DeCasien, S. A. Williams, and J. P. Higham. Primate brain size is predicted by diet but not sociality. *Nat. ecol. evol.* 1.5 (2017), 112. DOI: [10.1038/s41559-017-0112](https://doi.org/10.1038/s41559-017-0112).
- [45] M. Grabowski, B. T. Kopperud, M. Tsuboi, and T. F. Hansen. Both diet and sociality affect primate brain-size evolution. *Syst. biol.* 72.2 (2023), 404–418. DOI: [10.1093/sysbio/syac075](https://doi.org/10.1093/sysbio/syac075).
- [46] M. A. Brockhurst, A. Buckling, and A. Gardner. Cooperation peaks at intermediate disturbance. *Curr. biol.* 17.9 (2007), 761–5. DOI: [10.1016/j.cub.2007.02.057](https://doi.org/10.1016/j.cub.2007.02.057).
- [47] S. Miller and J. Knowles. Population fluctuation promotes cooperation in networks. *Sci. rep.* 5 (2015), 11054. DOI: [10.1038/srep11054](https://doi.org/10.1038/srep11054).
- [48] C. S. Gokhale and C. Hauert. Eco-evolutionary dynamics of social dilemmas. *Theor. popul. biol.* 111 (2016), 28–42. DOI: [10.1016/j.tpb.2016.05.005](https://doi.org/10.1016/j.tpb.2016.05.005).
- [49] V. Stojkoski, M. Karbevski, Z. Utkovski, L. Basnarkov, and L. Kocarev. Evolution of cooperation in networked heterogeneous fluctuating environments. *Physica a* 572 (2021), 125904. DOI: [10.1016/j.physa.2021.125904](https://doi.org/10.1016/j.physa.2021.125904).
- [50] D. Kroumi, É. Martin, C. Li, and S. Lessard. Effect of variability in payoffs on conditions for the evolution of cooperation in a small population. *Dyn. games appl.* 11.4 (2021), 803–34. DOI: [10.1007/s13235-021-00383-2](https://doi.org/10.1007/s13235-021-00383-2).
- [51] J. M. Borg and A. Channon. Testing the variability selection hypothesis: the adoption of social learning in increasingly variable environments. *Artificial life* 13. MIT Press, 2012, 317–324. DOI: [10.1162/978-0-262-31050-5-ch042](https://doi.org/10.1162/978-0-262-31050-5-ch042).
- [52] M. Assaf, M. Mobilia, and E. Roberts. Cooperation dilemma in finite populations under fluctuating environments. *Phys. rev. lett.* 111 (2013), 238101. DOI: [10.1103/PhysRevLett.111.238101](https://doi.org/10.1103/PhysRevLett.111.238101).
- [53] M. Pereda, D. Zurro, J. I. Santos, I. Briz I Godino, M. Álvarez, J. Caro, et al. Emergence and evolution of cooperation under resource pressure. *Sci. rep.* 7 (2017), 45574. DOI: [10.1038/srep45574](https://doi.org/10.1038/srep45574).

- [54] A. Szolnoki and X. Chen. Environmental feedback drives cooperation in spatial social dilemmas. *Epl* 120 (2017), 58001. DOI: [10.1209/0295-5075/120/58001](https://doi.org/10.1209/0295-5075/120/58001).
- [55] J. Huang, Y. Zhu, D. Zhao, C. Xia, and M. Perc. The impact of feedbacks on evolutionary game dynamics in structured populations. *Chaos* 35.6 (2025), 063134. DOI: [10.1063/5.0278673](https://doi.org/10.1063/5.0278673).
- [56] M. Inaba and E. Akiyama. Environmental variability promotes the evolution of cooperation among geographically dispersed groups on dynamic networks. *Plos complex syst.* 2.4 (2025), e0000038. DOI: [10.1371/journal.pcsy.0000038](https://doi.org/10.1371/journal.pcsy.0000038).
- [57] D. W. Bird, R. B. Bird, B. F. Codding, and D. W. Zeanah. Variability in the organization and size of hunter-gatherer groups: foragers do not live in small-scale societies. *J. hum. evol.* 131 (2019), 96–108. DOI: [10.1016/j.jhevol.2019.03.005](https://doi.org/10.1016/j.jhevol.2019.03.005).
- [58] R. I. M. Dunbar. Structure and function in human and primate social networks: implications for diffusion, network stability and health. *Proc. math. phys. eng. sci.* 476.2240 (2020), 20200446. DOI: [10.1098/rspa.2020.0446](https://doi.org/10.1098/rspa.2020.0446).
- [59] J. M. Smith. Group selection. *Q. rev. biol.* 51.2 (1976), 277–283. DOI: [10.1086/409311](https://doi.org/10.1086/409311).
- [60] S. Okasha. Why won't the group selection controversy go away? *Br. j. philos. sci.* 52.1 (2001), 25–50. DOI: [10.1093/bjps/52.1.25](https://doi.org/10.1093/bjps/52.1.25).
- [61] O. T. Eldakar and D. S. Wilson. Eight criticisms not to make about group selection. *Evolution* 65.6 (2011), 1523–1526. DOI: [10.1111/j.1558-5646.2011.01290.x](https://doi.org/10.1111/j.1558-5646.2011.01290.x).
- [62] C. K. W. De Dreu and Z. Triki. Intergroup conflict: origins, dynamics and consequences across taxa. *Philos. trans. r. soc. lond. b biol. sci.* 377.1851 (2022), 20210134. DOI: [10.1098/rstb.2021.0134](https://doi.org/10.1098/rstb.2021.0134).
- [63] A. M. M. Rodrigues, J. L. Barker, and E. J. H. Robinson. The evolution of intergroup cooperation. *Philos. trans. r. soc. lond. b biol. sci.* 378.1874 (2023), 20220074. DOI: [10.1098/rstb.2022.0074](https://doi.org/10.1098/rstb.2022.0074).
- [64] C. W. Marean. Pinnacle point cave 13B (Western Cape Province, South Africa) in context: The Cape Floral kingdom, shellfish, and modern human origins. *J. hum. evol.* 59.3-4 (2010), 425–443. DOI: [10.1016/j.jhevol.2010.07.011](https://doi.org/10.1016/j.jhevol.2010.07.011).
- [65] L. Wadley, C. Sievers, M. Bamford, P. Goldberg, F. Berna, and C. Miller. Middle Stone Age bedding construction and settlement patterns at Sibudu, South Africa. *Science* 334.6061 (2011), 1388–1391. DOI: [10.1126/science.1213317](https://doi.org/10.1126/science.1213317).
- [66] A. W. Kandel and N. J. Conard. Settlement patterns during the Earlier and Middle Stone Age around Langebaan Lagoon, Western Cape (South Africa). *Quat. int.* 270 (2012), 15–29. DOI: [10.1016/j.quaint.2011.06.038](https://doi.org/10.1016/j.quaint.2011.06.038).

- [67] K. Hasselmann. Stochastic climate models: part I. theory. *Tellus a* 28.6 (1976), 473. DOI: [10.3402/tellusa.v28i6.11316](https://doi.org/10.3402/tellusa.v28i6.11316).
- [68] D. Vyushin, P. Kushner, and F. Zwiers. Modeling and understanding persistence of climate variability. *J geophys res* 117.D21 (2012). DOI: [10.1029/2012JD018240](https://doi.org/10.1029/2012JD018240).
- [69] S. Salcedo-Sanz, D. Casillas-Pérez, J. Del Ser, C. Casanova-Mateo, L. Cuadra, M. Piles, et al. Persistence in complex systems. *Phys. rep.* 957 (2022), 1–73. DOI: [10.1016/j.physrep.2022.02.002](https://doi.org/10.1016/j.physrep.2022.02.002).
- [70] G. Hardin. The tragedy of the commons: the population problem has no technical solution; it requires a fundamental extension in morality. *Science* 162.3859 (1968), 1243–1248. DOI: [10.1126/science.162.3859.1243](https://doi.org/10.1126/science.162.3859.1243).
- [71] K. G. Binmore. Game theory and the social contract: just playing. Vol. 2. MIT press, 1994.
- [72] P. Kollock. Social dilemmas: the anatomy of cooperation. *Annu. rev. sociol.* 24 (1998), 183–214. DOI: [10.1146/annurev.soc.24.1.183](https://doi.org/10.1146/annurev.soc.24.1.183).
- [73] F. C. Santos, M. D. Santos, and J. M. Pacheco. Social diversity promotes the emergence of cooperation in public goods games. *Nature* 454.7201 (2008), 213–216. DOI: [10.1038/nature06940](https://doi.org/10.1038/nature06940).
- [74] F. C. Santos and J. M. Pacheco. Scale-free networks provide a unifying framework for the emergence of cooperation. *Phys. rev. lett.* 95.9 (2005), 098104. DOI: [10.1103/PhysRevLett.95.098104](https://doi.org/10.1103/PhysRevLett.95.098104).
- [75] F. C. Santos, J. M. Pacheco, and T. Lenaerts. Evolutionary dynamics of social dilemmas in structured heterogeneous populations. *Proc. natl. acad. sci. u. s. a.* 103.9 (2006), 3490–3494. DOI: [10.1073/pnas.0508201103](https://doi.org/10.1073/pnas.0508201103).
- [76] Y. Meng, S. P. Cornelius, Y.-Y. Liu, and A. Li. Dynamics of collective cooperation under personalised strategy updates. *Nat. commun.* 15.1 (2024), 3125. DOI: [10.1038/s41467-024-47380-8](https://doi.org/10.1038/s41467-024-47380-8).
- [77] L. A. Dugatkin and D. S. Wilson. Rover: a strategy for exploiting cooperators in a patchy environment. *Am. nat.* 138.3 (1991), 687–701. DOI: [10.1086/285243](https://doi.org/10.1086/285243).
- [78] M. H. Vainstein and J. J. Arenzon. Disordered environments in spatial games. *Phys. rev. e stat. nonlinear. soft matter phys.* 64.5 Pt 1 (2001), 051905. DOI: [10.1103/PhysRevE.64.051905](https://doi.org/10.1103/PhysRevE.64.051905).
- [79] M. H. Vainstein, A. T. C. Silva, and J. J. Arenzon. Does mobility decrease cooperation? *J. theor. biol.* 244.4 (2007), 722–8. DOI: [10.1016/j.jtbi.2006.09.012](https://doi.org/10.1016/j.jtbi.2006.09.012).

- [80] C. Liu, J. Wang, X. Li, and C. Xia. The link weight adjustment considering historical strategy promotes the cooperation in the spatial prisoner's dilemma game. *Physica a* 554.124691 (2020), 124691. DOI: [10.1016/j.physa.2020.124691](https://doi.org/10.1016/j.physa.2020.124691).
- [81] X. Xiong, Z. Zeng, M. Feng, and A. Szolnoki. Coevolution of relationship and interaction in cooperative dynamical multiplex networks. *Chaos* 34.2 (2024), 023118. DOI: [10.1063/5.0188168](https://doi.org/10.1063/5.0188168).
- [82] M. Inaba and E. Akiyama. Evolution of cooperation among migrating resource-oriented agents under environmental variability. *Chaos, solitons & fractals* 202 (2025), 117592. DOI: [10.1016/j.chaos.2025.117592](https://doi.org/10.1016/j.chaos.2025.117592).
- [83] R. Cong, B. Wu, Y. Qiu, and L. Wang. Evolution of cooperation driven by reputation-based migration. *Plos one* 7.5 (2012), e35776. DOI: [10.1371/journal.pone.0035776](https://doi.org/10.1371/journal.pone.0035776).
- [84] X. Chen, A. Szolnoki, and M. Perc. Risk-driven migration and the collective-risk social dilemma. *Phys. rev. e* 86 (2012), 036101. DOI: [10.1103/PhysRevE.86.036101](https://doi.org/10.1103/PhysRevE.86.036101).
- [85] Z. He, Y. Geng, C. Shen, and L. Shi. Evolution of cooperation in the spatial prisoner's dilemma game with extortion strategy under win-stay-lose-move rule. *Chaos solitons fractals* 141 (2020), 110421. DOI: [10.1016/j.chaos.2020.110421](https://doi.org/10.1016/j.chaos.2020.110421).
- [86] S. Dhakal, R. Chiong, M. Chica, and R. H. Middleton. Climate change induced migration and the evolution of cooperation. *Appl. math. comput.* 377 (2020), 125090. DOI: [10.1016/j.amc.2020.125090](https://doi.org/10.1016/j.amc.2020.125090).
- [87] T. Ren and J. Zheng. Evolutionary dynamics in the spatial public goods game with tolerance-based expulsion and cooperation. *Chaos solitons fractals* 151 (2021), 111241. DOI: [10.1016/j.chaos.2021.111241](https://doi.org/10.1016/j.chaos.2021.111241).
- [88] Y. Yang, Q. Pan, and M. He. The influence of environment-based autonomous mobility on the evolution of cooperation. *Chaos solitons fractals* 169 (2023), 113320. DOI: [10.1016/j.chaos.2023.113320](https://doi.org/10.1016/j.chaos.2023.113320).
- [89] H. Zhang. Evolution of cooperation among fairness-seeking agents in spatial public goods game. *Appl. math. comput.* 489 (2025), 129183. DOI: [10.1016/j.amc.2024.129183](https://doi.org/10.1016/j.amc.2024.129183).
- [90] B. A. Huberman and N. S. Glance. Evolutionary games and computer simulations. *Proc. natl. acad. sci. u.s.a.* 90.16 (1993), 7716–8. DOI: [10.1073/pnas.90.16.7716](https://doi.org/10.1073/pnas.90.16.7716).
- [91] G. Zhang, X. Xiong, B. Pi, M. Feng, and M. Perc. Spatial public goods games with queueing and reputation. *Appl. math. comput.* 505 (2025), 129533. DOI: [10.1016/j.amc.2025.129533](https://doi.org/10.1016/j.amc.2025.129533).
- [92] M. D. Cohen, R. L. Riolo, and R. Axelrod. The role of social structure in the maintenance of cooperative regimes. *Ration. soc.* 13.1 (2001), 5–32. DOI: [10.1177/104346301013001001](https://doi.org/10.1177/104346301013001001).

- [93] Z. Wang, L. Wang, A. Szolnoki, and M. Perc. Evolutionary games on multilayer networks: a colloquium. *Eur. phys. j. b* 88.5 (2015). DOI: [10.1140/epjb/e2015-60270-7](https://doi.org/10.1140/epjb/e2015-60270-7).
- [94] N. Masuda and R. Lambiotte. A guide to temporal networks. World Scientific, 2020.
- [95] M. Inaba and E. Akiyama. Evolution of cooperation in multiplex networks through asymmetry between interaction and replacement. *Sci. rep.* 13.1 (2023), 9814. DOI: [10.1038/s41598-023-37074-4](https://doi.org/10.1038/s41598-023-37074-4).
- [96] H.-W. Lee, C. Cleveland, and A. Szolnoki. When costly migration helps to improve cooperation. *Chaos* 32.9 (2022), 093103. DOI: [10.1063/5.0100772](https://doi.org/10.1063/5.0100772).
- [97] H. Ohtsuki and S. Ujiyama. Impact of social dominance on the evolution of individual learning. *J. theor. biol.* 535 (2022), 110986. DOI: [10.1016/j.jtbi.2021.110986](https://doi.org/10.1016/j.jtbi.2021.110986).
- [98] M. A. Turner, C. Moya, P. E. Smaldino, and J. H. Jones. The form of uncertainty affects selection for social learning. *Evol. hum. sci.* 5 (2023), e20. DOI: [10.1017/ehs.2023.11](https://doi.org/10.1017/ehs.2023.11).
- [99] B. Pi, L.-J. Deng, M. Feng, M. Perc, and J. Kurths. Dynamic evolution of complex networks: a reinforcement learning approach applying evolutionary games to community structure. *Ieee trans. pattern anal. mach. intell.* 47.10 (2025), 8563–82. DOI: [10.1109/TPAMI.2025.3579895](https://doi.org/10.1109/TPAMI.2025.3579895).

Acknowledgments

I would like to express my gratitude to those who contributed to the completion of this dissertation.

First and foremost, I wish to thank my primary supervisor, Professor Eizo Akiyama, for his guidance throughout my five years of doctoral studies. During the formative stages of my graduate education, he provided a necessary foundation in the principles and methodology of scholarly research. I am especially grateful for his consistent engagement with my research; he remained the first to understand my ideas, at times a rigorous critic, and always a dedicated supporter. I also acknowledge his contributions as a co-author of the two published articles that form the basis of this dissertation.

I am also grateful to my secondary supervisors, Professor Ryoji Sawa and Professor Tuan Phung-Duc, for their critical questions and constructive advice. Their feedback provided an invaluable opportunity to further deepen the discussion and insights of this study.

Furthermore, I would like to thank the members of the examination committee for their insightful comments. I am grateful to Assistant Professor Hidekazu Anno for providing critical feedback from the perspective of an expert outside the field of study, which helped situate the research within a broader academic context. I also thank Professor Hitoshi Yamamoto, whose extensive knowledge and experience in the evolution of cooperation proved indispensable in refining the theoretical rigor and academic significance of this work.

Finally, I acknowledge the institutional and academic support provided by the University of Tsukuba, which made this research possible.